Spatial correlations in dark energy and their effects on strong gravitational lenses

Mahir C. Erciyas

September 27, 2023

First supervisor: dr. E. Chisari
Second supervisor: dr. T. Prokopec
Daily supervisor: dr. E. Belgacem

Institute for Theoretical Physics
Utrecht University

September, 2023

Utrecht University

Abstract

The accelerating expansion of our universe is currently theorized to be driven by dark energy, of which the nature is yet a mystery. In this thesis, we investigate the possibility of fluctuations in dark energy and resulting spatial correlations. These fluctuations carry through into the Hubble parameter, affecting cosmological observables. We show that time delays of strong gravitational lenses are dressed by this effect, and correlators of said time delays acquire an angular dependence. To investigate this angular dependence, we construct the angular power spectrum of time delay correlators. Subsequently, we hone in on a specific realization of a fluctuating dark energy density, considering quantum fluctuations of a light scalar field in the early universe and their subsequent imprinted spatial correlations today. We then perform a forecast using a mock dataset for the upcoming Legacy Survey of Space and Time (LSST), comparing the effect to correlations of weak gravitational lenses in regular ΛCDM.

Contents

1 Introduction

Cosmology entails the study of the structure and history of our universe. Currently, there are several well-tested theories that individually describe the matter content and geometric features of said universe. Of these theories, the ones considered the best are the Standard Model of particle physics which describes matter, and general relativity which describes the geometry of space-time. Notwithstanding, observational data going back as far as the 1930s [1–3] suggests that the Standard Model requires additional components – such as dark matter and dark energy (although these components could be explained within the bounds of the Standard Model by means of a cosmological constant and a weakly interacting massive particle (WIMP), these descriptions have their own flaws) – in order to accurately describe features like galactic clustering and the accelerating expansion of our universe. This leads to the currently most widely accepted model of cosmology, ΛCDM.

ΛCDM derives its name from the aforementioned additional components, namely cold dark matter (CDM), and the cosmological constant Λ, often referred to as dark energy. In this paper, the focus will be on dark energy, which is the component that drives the accelerating expansion of the universe. This accelerating expansion was initially observed in measurements of Type 1A supernovae [4], and later the cosmic microwave background (CMB) [5]. Although the addition of dark energy to the previously flawed models ameliorates some of the mismatches between theory and experiment, the nature of this component is unknown. In fact, the peculiar properties of dark energy- namely a negative pressure and and a non-diluting energy density- only further highlight this issue. As of now, most theories introduce dark energy in the form of some scalar field, for example quintessence [6] or k-essence [7]. However, qualms with existing theories and the generally mysterious nature of dark energy have led to a wide variety of models that are different in nature, such as modified gravity [8, 9].

To add to the already existing woes of dark energy, it turns out that its mere inclusion is not enough to rid the model of all of its statistical tensions. In fact, the cosmological parameters that are experimentally probed at various scales, most notably the Hubble parameter H_0 and the present matter fluctuation parameter σ_8, have tensions of up to 5σ [10] and 3σ [5], respectively. To many, this indicates the presence of physics beyond what ΛCDM can account for. There exist works that attempt to resolve the Hubble tension by means of early dark energy considerations [11, 12]. However, a slightly different approach will be taken in this paper, where the focus will be on the spatial correlations of dark energy.

Our universe is rife with spatial correlations. We can observe them in the temperature fluctuations of our CMB [13], the distribution of galaxies in the sky [14], and in light wave noise [15]. The origin of all these correlations is quantum mechanical in nature, which suggests a strong connection between the observed structure of our universe, and the quantum effects underlying it all.

Considering this precedent, it is not unreasonable to assume that dark energy itself is quantum mechanical in nature. In practice, this means that dark energy is characterized by a fluctuating (scalar) field, composite or fundamental. In fact, that will be perspective taken in this body of work, where dark energy fluctuations are sourced by either a massless or very light scalar field that is spectator during inflation. Models with fluctuations of this origin have been previously explored in [16–19]. In the aforementioned works, the introduction of said fluctuations was able to diminish the Hubble tension down to 1σ.

Given the upcoming body of new data that will be provided by the Large Synoptic Survey Telescope (LSST) [20], we will soon have the capability to rule out some of the large amount of models of inflation that currently exist. Consequently, it is meritable to also consider the theoretical predictions of this specific class of models. Naturally, one must then consider how dark energy fluctuations affect physical observables.

Therefore, one must derive the Friedmann equations in this context, i.e. in operator form. This leads to the following expression:

$$3M_p^2\hat{H}^2(z,\hat{n}) = \rho_C(z)\hat{I} + \hat{\rho}_Q(z,\hat{n}), \tag{1.1}$$

with $M_p = 2.435 \cdot 10^{18}$ GeV/c^2 the reduced Planck mass, ρ_C the energy density of classical matter, $\hat{\rho}_Q$ the energy density operator of the dark energy field, and $\hat{I}$ the identity operator. This operator equation can be derived in ADM formalism [21], by taking the gradient expansion of the energy constraint. Note the

introduction of the unit vector in the celestial sphere, $\hat{n}$, which appears due to the consideration of spatial correlations.

Naturally, the introduction of this fluctuating Hubble rate has consequences for physical observables. In this paper, we will focus on how these fluctuations will dress the time delays of strong lenses. Although this will be detailed further in section 4, it is notable that these fluctuations will enter by means of the angular diameter distance. This, in ΛCDM, has the expression

$$D_{ij}(z_i, z_j) = (1 + z_j) \int_{z_i}^{z_j} dz' H^{-1}(z') \tag{1.2}$$

in terms of the redshift z, but is now realized by the operator description with directional dependence

$$\hat{D}_{ij}(z_i, z_j, \hat{n}) = (1 + z_j) \int_{z_i}^{z_j} dz' \hat{H}^{-1}(z', \hat{n}) \tag{1.3}$$

through the fluctuating Hubble operator $\hat{H}(z', \hat{n})$. Consequently, this will also affect time delays due to strong gravitational lenses, which are proportional to several angular diameter distances:

$$\tau(\vec{\theta}, \vec{\beta}) = \frac{1 + z_l}{c} \frac{D_l D_s}{D_{ls}} \left[\frac{(\vec{\theta} - \vec{\beta})^2}{2} - \psi(\vec{\theta}) \right]. \tag{1.4}$$

Herein, c is the speed of light, z_l is the redshift of the lens, $\vec{\theta}$ is the observed angular position of the source, $\vec{\beta}$ is the unlensed angular position of the source, and D_l, D_s and D_{ls} are the angular diameter distances from us to the lens, from us to the source, and from the lens to the source, respectively. We will derive the full expression for this dressed time delay, and consider some of the behaviour of common strong gravitational lens models under the effects of these fluctuations.

Additionally, we will consider a source of noise, namely contaminants from weak gravitational lenses, and note to what extent they may mask the dark energy fluctuations.

To this end, the thesis is be organized as follows. In section 2, we describe the current state of cosmology and give some information about lensing formalism. One acquainted with cosmology could skip this section. In section 3, we describe a phenomenological model which contains spatial correlations in the dark energy density. Subsequently, we calculate how these effects carry through into the time delays of images of strong gravitational lenses in section 4. In section 5, we connect these dressed expressions to the angular power spectra that we observe in the sky when doing surveys. We then consider weak gravitational lensing as a contaminant on top of these angular power spectra in section 6. Having derived the required expressions, we can then calculate values by using mock datasets of upcoming surveys. These datasets and the adjustments we make to them are detailed in section 7. We then show our results for the weak lensing contaminant in section 8. In section 9, we slightly change paces by detailing a specific realization of the phenomenological model that we previously discussed. In doing so, we acquire several model parameters, based on which we detail the parameter ranges that we are interested in in section 10. Finally, we summarize, conclude and have a short discussion on the future prospects of this model in section 11. Some of the more involved calculations are then given in the appendices.

2 General Cosmology

Cosmology is the study of the universe as a whole. Although this is a challenging matter, recent developments in both formalism and survey technology have allowed us to make remarkable strides in our understanding of the cosmos and its evolution.

One cornerstone of modern cosmology is the so-called ΛCDM model, which describes a universe with dark energy, denoted Λ, and cold dark matter – CDM. This model has allowed us to describe the cosmic microwave background and large scale structure that we observe to great success. However, ΛCDM is not without its flaws, as several parameters of the model display statistical tensions when probed at different scales.

In addition, modern cosmology generally assumes the theory of inflation – a period of rapid expansion in the early universe. This is yet another cornerstone, however, we are woefully unaware of whether this theory represents the reality, as the ultimate (observational) tests of inflation are still lacking.

Add to this the peculiar nature of both dark matter and dark energy, which are postulated to, respectively, make up 27% and 68% of the total energy content of the universe despite having an unknown physical origin and only having been observed through their gravitational effects, and it is easy to see why cosmology is an active field of physics.

2.1 Standard definitions

We will first introduce some of the standard concepts and definitions used in all of cosmology. One that is already familiar with the field could skip this section. Most of this theory is based on [22] and further detailed there.

From observational evidence, we know that the universe is expanding. We quantify said expansion of physical length scales by means of the so-called scale factor a. This may seem haphazard, but this scale factor can also be motivated physically as the ratio of wavelengths λ between emitted and observed photons: due to the expanding universe, the Doppler effect causes emitted photons from objects that are further away from us to appear higher-wavelength than they are. Physically, this means a shift towards the red end of the visible light spectrum, and is denoted by the redshift z:

$$\frac{\lambda_{obs}}{\lambda_{emit}} \equiv \frac{1}{a_{emit}} = 1 + z_{emit}. \tag{2.1}$$

Note that this implies that for the current value of the scale factor, $a_{obs} = 1$. Additionally note that the redshift z is directly proportional to this ratio rather than inversely. Because physical distances are ever-increasing, it would be useful to have a universal length scale that is expansion-invariant. To this end, we first define the Hubble parameter, which encodes the (logarithmic) rate of change of the scale factor:

$$H(t) \equiv \frac{d(\ln(a(t)))}{dt} = \frac{\dot{a}(t)}{a(t)}. \tag{2.2}$$

It is notable that both the scale factor and redshift encode a timescale, namely one that holds more relevance in the context of an expanding universe. As such, we will see these come back quite often. In order to derive the aforementioned expansion-invariant length scale, we will first need more information about the shape of spacetime. To this end, one must define a metric $g_{\mu\nu}$ where $\mu, \nu = 0, \ldots, 3$ denote spacetime indices. It turns out that for a universe that is approximately homogenous and isotropic at large scales, not unlike ours, the Friedmann-Lemaître-Robertson-Walker (FLRW) metric suffices. It gives rise to the following invariant line element,

$$ds^2(x) = \sum_{\mu,\nu=0}^{3} g_{\mu\nu} dx^\mu dx^\nu = -dt^2 + a^2(t)\delta_{ij} dx^i dx^j,$$

where t denotes cosmic time and x^i denote the three spatial components. Note that the scale factor very literally scales the spatial components as a pre-factor in this metric. It is also important to note that any

partial derivatives will now have to account for the structure of spacetime imposed by the FLRW metric. To this end, we define the covariant derivative

$$\nabla_\mu T^\alpha = \partial_\mu T^\alpha + \Gamma^\alpha_{\mu\nu} T^\nu, \tag{2.3}$$

where T^α is some rank one tensor and $\Gamma^\alpha_{\mu\nu}$ is the Christoffel symbol

$$\Gamma^\alpha_{\mu\nu} = \frac{1}{2} g^{\alpha\sigma}(\partial_\mu g_{\sigma\nu} + \partial_\nu g_{\mu\sigma} - \partial_\sigma g_{\mu\nu}), \tag{2.4}$$

which acts as the torsion-free Levi-Civita connection of a metric in general relativity (GR). The derivations and deeper meaning behind these definitions are beyond the scope of this thesis, but can be found in any source on differential geometry. We can now vary and minimize the Einstein-Hilbert action coupled to the matter action,

$$S_{EH} + S_m = \frac{1}{16\pi G_N} \int d^4x \sqrt{-g}\mathcal{R} + S_m, \tag{2.5}$$

where $g = \det(g_{\mu\nu})$, G_N is the gravitational constant, and $\mathcal{R}$ is the Ricci curvature scalar. This gives rise to the well-known Einstein field equations,

$$G_{\mu\nu}(x) \equiv \mathcal{R}_{\mu\nu}(x) - \frac{1}{2} g_{\mu\nu}(x)\mathcal{R}(x) = 8\pi G_N T_{\mu\nu}(x), \tag{2.6}$$

where $G_{\mu\nu}$ is the Einstein tensor, $\mathcal{R}_{\mu\nu}$ the Ricci tensor, and $T_{\mu\nu}$ the energy-momentum tensor. Note that these equations relate the energy content of the universe to its geometric features. In particular, $\mathcal{R}_{\mu\nu}$ and $g_{\mu\nu}\mathcal{R}$ describe the curvature of the universe, and $T_{\mu\nu}$ encodes the energy content of the universe.

Plugging in the aforementioned FLRW metric allows us to compute the components of the Ricci tensor, namely

$$\mathcal{R}_{00} = -3\frac{\ddot{a}}{a}, \tag{2.7}$$

$$\mathcal{R}_{ij} = \delta_{ij}[2\dot{a}^2 + a\ddot{a}]. \tag{2.8}$$

The Ricci scalar then naturally follows:

$$\mathcal{R} \equiv R_{\mu\nu} g^{\mu\nu} = 6\left[\frac{\ddot{a}}{a} + \left(\frac{\dot{a}}{a}\right)^2\right]. \tag{2.9}$$

We will now assume that the energy-momentum tensor is sourced by an ideal fluid, i.e. $T^0{}_0 = -\rho$ and $T^i{}_j = \delta^i{}_j \mathcal{P}$. Here, ρ represents the energy density from all species: matter, radiation, and dark energy- and $\mathcal{P}$ the corresponding momenta.

We now have all the necessary components to calculate the solutions of the Einstein field equations:

$$H^2(t) = \frac{8\pi G_N}{3}\rho(t), \tag{2.10}$$

$$\frac{\ddot{a}}{a}(t) = -\frac{4\pi G_N}{3}(\rho(t) + 3\mathcal{P}(t)). \tag{2.11}$$

Enforcing energy-momentum conservation in the FLRW spacetime gives us one more equation, namely

$$\dot{\rho}(t) + 3H(t)(\rho(t) + \mathcal{P}(t)) = 0. \tag{2.12}$$

We will now assume that the energy-momentum tensor is sourced by an ideal fluid with the equation of state $\mathcal{P} = w\rho$. This ideal fluid will have several components, namely dust and dark matter ($w = 0$), relativistic matter ($w = 1/3$) and a cosmological constant ($w = -1$). We can now rewrite the Friedmann equations as

$$\frac{H^2(t)}{H_0^2} = \Omega_m a^{-3}(t) + \Omega_R a^{-4}(t) + \Omega_\Lambda$$

$$= \Omega_m(1+z(t))^3 + \Omega_r(1+z(t))^4 + \Omega_\Lambda, \tag{2.13}$$

where H_0 is the Hubble parameter today and $\Omega_i = \frac{8\pi G_N}{3H_0^2}\rho_i$ are the dimensionless energy density fractions of the various species today. These have been measured to be approximately $\Omega_m = 0.315$ and $\Omega_\Lambda = 0.685$, with $\Omega_R \sim 10^{-4}$ being comparitively small [5]. It is notable that although Ω_R is extremely small today, its dependence on $a^{-4}(t)$ means that it was the dominant density fraction in the very early universe. Conversely, Ω_m was comparatively small. The period at which these two densities were equal is denoted the epoch of matter-radiation equality, and is known to be at $z_{eq} \approx 3400$.

Now that we know what the evolution of $H(t)$ looks like in theory, we can define the comoving distance, which is the aforementioned expansion-invariant length scale:

$$\chi(z) = \int_0^{a(z)} \frac{d\ln a'(z)}{a'(z)H(a'(z))} = c\int_0^z \frac{dz'}{H(z')}. \tag{2.14}$$

We chose to express $\chi(z)$ in terms of the redshift for later convenience. It is notable that $\chi(z)$ depends entirely on the evolution of the Hubble parameter. In fact, a shrinking factor $\frac{1}{aH}$ implies that $\ddot{a} > 0$: an accelerating expansion of the universe. The period of accelerating expansion in the early universe is the epoch that we refer to as inflation. We also define the luminosity distance

$$d_L(z) = (1+z)\chi(z), \tag{2.15}$$

which we note only differs by a factor $1+z$. It is notable that the luminosity distance has an intuitive derivation based off the measured flux of an object of known luminosity, which is detailed in Appendix A.

The formalism established up until now serves to describe inflation. However, all of this does not cover the full picture. Namely, the presence of inflation is precisely what allows us to describe the imprints of quantum fluctuations from the early universe in the cosmic microwave background that we can observe today. These fluctuations originate from inflation, after which they are imprinted into the cosmic microwave background.

We describe these imprinted quantum fluctuations and our observations of them by means of the so-called power spectra. In particular, matter perturbations are quantified using the density perturbation δ. These δ can be understood to be matter overdensities described by the deviation from the average density $\bar{\rho}$:

$$\delta(\vec{k}, z) = \frac{\rho(\vec{k}, z) - \bar{\rho}(z)}{\bar{\rho}(z)}. \tag{2.16}$$

The statistical properties of these δ are then described by its two-point function, but also higher order n-point functions. The two-point functions in particular are denoted the matter power spectrum P_m:

$$\langle \delta(\vec{k}, z)\delta^*(\vec{k}', z')\rangle = (2\pi)^3 P_m(k, z, z')\delta(\vec{k} - \vec{k}'). \tag{2.17}$$

Note that δ as seen in $\langle \dots \rangle$ are matter overdensities, but the δ on the right-hand side is a Kronecker delta. We can understand that the matter power spectrum is, by construction, the Fourier transformed correlation function of matter overdensities. We typically linearize the matter power spectrum in time, as we are only interested in its region of linear growth – these are the long-wavelength parts, for which an initial Gaussian power spectrum evolves into a Gaussian power spectrum. We do this by means of linear growth functions $D_1(z)$ such that

$$P_m(k, z, z') = D_1(z)D_1(z')P_{m,0}(k), \tag{2.18}$$

where $P_{m,0}$ is the matter power spectrum today. We can further extend this formalism to other fields and potentials. In particular, we will later see that we can consider correlators of the gravitational potential $\tilde{\Phi}(\vec{k}, z)$, giving us a weak lensing power spectrum

$$\langle \tilde{\Phi}(\vec{k}, z), \tilde{\Phi}(\vec{k}', z')\rangle = (2\pi)^3 P_\Phi(k, z, z')\delta(\vec{k} - \vec{k}'). \tag{2.19}$$

The origins of these potentials will be explained in subsection 2.3. It is notable that this power spectrum relates to the matter power spectrum due to the following relation:

$$\tilde{\Phi}(\vec{k}, a) = \frac{4\pi G\rho_m(a)\tilde{\delta}(\vec{k})}{k^2}, \tag{2.20}$$

which stems from the Poisson equation

$$\nabla^2\Phi = 4\pi G\rho \tag{2.21}$$

transformed into momentum space.

2.2 Strong lensing

As one may expect from a mere glance at the Einstein field equations, objects with large energy densities, such as galaxy clusters, can give rise to considerable local curvature in spacetime. This is what causes strong lensing- Incoming photons from a foreign object move through a distorted patch of spacetime, giving rise to observed images that are shifted in position, distorted, or multiplied, i.e. several images of a single object. Although the Einstein field equations detailing these effects are heavily non-linear, lensing is typically described in a Newtonian manner. Namely, one uses a linear equation in the form of the lens equation,

$$\vec{\beta} = \vec{\theta} - \vec{\alpha}(\vec{\theta}), \tag{2.22}$$

as defined in [23]. Herein, $\vec{\beta}$ is the angular position of the source pre-lensing, $\vec{\theta}$ the angular position post-lensing, and $\vec{\alpha}$ the deflection angle. This is further depicted in Figure 2.1.

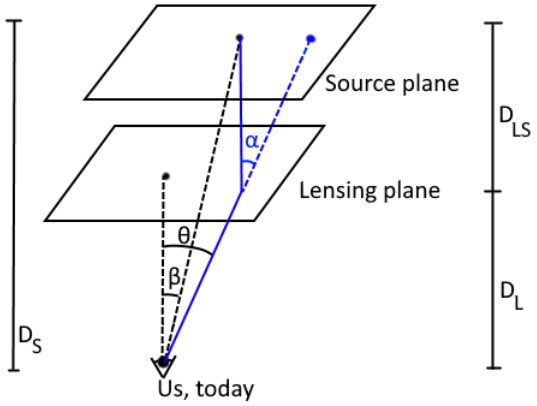

Figure 2.1: Photons from a source get strongly lensed, giving rise to an image at an angle α from the source relative to the lensing plane. Note that the angular diameter distances used in (2.27) are also depicted here.

There exists a lensing potential ψ of which the gradient gives rise to the deflection angle

$$\vec{\nabla}\psi(\vec{\theta}) = \vec{\alpha}(\vec{\theta}). \tag{2.23}$$

This potential, in turn, is defined by the so-called convergence κ, which is determined by the properties of the strong lens and relates to the potential by means of a Poisson equation

$$\kappa(\vec{\theta}) = \frac{1}{2}\nabla^2\psi(\vec{\theta}). \tag{2.24}$$

This convergence is essentially a 2D-projected mass distribution. We can alternatively express this in terms of the gravitational potential Φ and mass density ρ,

$$4\pi G\rho(\vec{r}) = \nabla^2\Phi(\vec{r}). \tag{2.25}$$

When an object is strongly lensed, the photon path from said object is curved, naturally extending the travel time of the photons. This is the so-called (dimensionless) time delay, which can be expressed in terms of the

lensing potential as follows

$$\tau(\vec{\theta},\vec{\beta}) \equiv \left[\frac{(\vec{\theta}-\vec{\beta})^2}{2} - \psi(\vec{\theta})\right] = \left[\frac{(\vec{\nabla}_\theta\psi)^2}{2} - \psi(\vec{\theta})\right]. \tag{2.26}$$

This dimensionless time delay, also denoted the Fermat potential, can now be used to calculate the relative arrival time of two images. In order to do this, one must first scale this value by the time-delay distance

$$D_{\Delta t} \equiv (1+z_l)\frac{D_l D_s}{D_{ls}}, \tag{2.27}$$

which is given in terms of angular diameter distances $D(z)(1+z)^2 = d_L(z)$. The relative time delay is then

$$\Delta t_{ab} = \frac{D_{\Delta t}}{c}[\tau(\vec{\theta}_a,\vec{\beta}) - \tau(\vec{\theta}_b,\vec{\beta})]. \tag{2.28}$$

2.2.1 Spherical lens profiles

For a singular isothermal sphere (SIS) defined by the three-dimensional mass density

$$\rho(\vec{r}) = \frac{\sigma_v^2}{2\pi G\vec{r}^2}, \tag{2.29}$$

with σ_v the velocity dispersion and distance $\vec{r}$, the Poisson equation gives us the gravitational potential Φ as follows:

$$\nabla^2\Phi = 4\pi G\rho \Rightarrow \Phi(\vec{r}) = 2\sigma_v^2 \ln\frac{\vec{r}}{r_0}. \tag{2.30}$$

By normalizing in terms of the constants $\frac{\sigma_v^2}{2\pi G}$, we can plot $\rho(\vec{r})$ as follows:

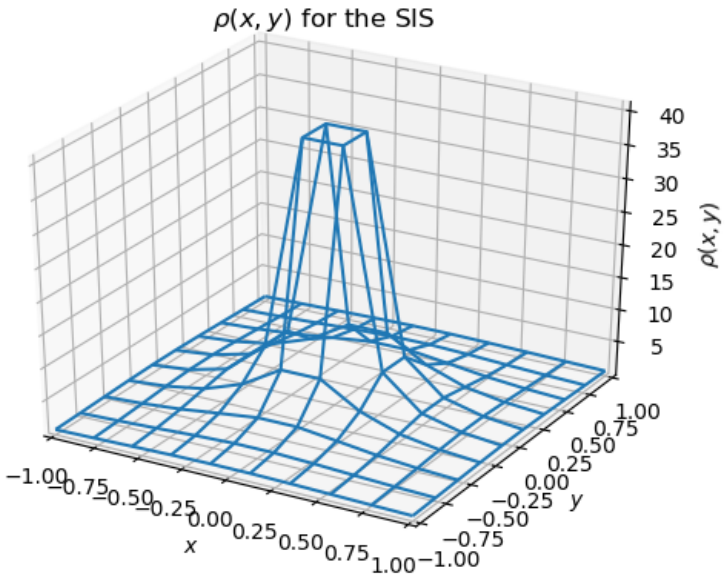

Figure 2.2: A depiction of $\rho(\vec{r})$ for the SIS where we set $z = 0$ for ease of visualization, – hence the dependence on solely x and y. Note that we rescaled the coordinates to get rid of all constant pre-factors. Further note that we see a ramp-up in $\rho(x, y)$ as we approach the singularity at $\vec{r} = \vec{0}$, which was omitted for obvious reasons.

We can split the coordinates up as $\vec{r}^2 = \vec{r}_\perp^2 + z^2$, where $\vec{r}_\perp$ gives the components $\vec{\theta}\chi$ in the plane perpendicular to the line-of-sight, i.e. the lens plane, and s gives the line-of-sight component χ. In order to reduce this expression down to a potential projected onto the two-dimensional plane, which is the part that we will effectively observe, we will integrate over the line-of-sight component z as follows:

$$\Theta(\vec{r}_\perp) = \int_{-\infty}^{\infty} \frac{dz}{c} \frac{\Phi(\vec{r})}{c^2}. \tag{2.31}$$

Herein, Θ is related to the lensing potential in the given way:

$$\psi = 2c \frac{D_{ls}}{D_l D_s} \Theta. \tag{2.32}$$

We can express (2.28) in terms of Θ as follows:

$$\Delta t_{ab} = \left[(\vec{\nabla}_\theta \Theta^{(a)})^2 - (\vec{\nabla}_\theta \Theta^{(b)})^2 - 2[\Theta^{(a)} - \Theta^{(b)}] \right]. \tag{2.33}$$

The integral in Θ can be divergent. However, as we can see in (2.33), we are not interested in the raw potentials, but merely the differences between them. Namely, if we consider the expression for the relative time delay, we find (see appendix B) that

$$\Theta^{(a)} - \Theta^{(b)} = \frac{2\pi\sigma_v^2}{c^3}(r_{\perp,a} - r_{\perp,b}). \tag{2.34}$$

Similarly, we can calculate that

$$(\vec{\nabla}_\perp \Theta)^2 = \frac{4\pi^2\sigma_v^4}{c^6}. \tag{2.35}$$

We note that this is a constant, so

$$(\vec{\nabla}_\perp \Theta^{(a)})^2 - (\vec{\nabla}_\perp \Theta^{(b)})^2 = 0. \tag{2.36}$$

We observe that the deflection angle terms vanish. This is a property unique to the SIS, and is what makes it the simplest option to consider. We can also analytically solve the lens equation to find the positions of the images. In order to do so, let us rewrite the lensing potential as

$$\psi(\vec{\theta}) = \theta_E \|\vec{\theta}\| + C, \tag{2.37}$$

where we defined the Einstein radius $\theta_E = \frac{D_{ls}}{D_s} \frac{4\pi\sigma_v^2}{c^2}$. For simplicity, we will rescale our coordinates $\vec{x} := \frac{\vec{\theta}}{\theta_E}$ and $\vec{y} := \frac{\vec{\beta}}{\theta_E}$, which gives the following lens equation

$$x_i - y_i = \frac{x_i}{\|\vec{x}\|}. \tag{2.38}$$

We now want to solve this for $\vec{x}$, which gives us

$$\vec{x}\left(1 - \frac{1}{\|\vec{x}\|}\right) = \vec{y}. \tag{2.39}$$

The reason why the Einstein radius is denoted a radius is now evident: when the source is directly behind the strong lens ($\vec{y} = \vec{0}$), the position of the image is given by a circle of radius θ_E around the lens. When $\vec{y} \neq \vec{0}$, we can note that the source and the images must be collinear. We therefore have $\vec{x} = \alpha\vec{y}$, with α some real constant. We can now discern two cases, namely

$$\alpha = \begin{cases} 1 + \frac{1}{||\vec{y}||} & \alpha > 0 \\ 1 - \frac{1}{||\vec{y}||} & \alpha < 0 \quad (||\vec{\beta}|| < \theta_E). \end{cases} \tag{2.40}$$

We can immediately conclude that we are only interested in the case where $||\vec{\beta}|| < \theta_E$, as we only get a deflection rather than two images when $||\vec{\beta}|| > \theta_E$. This is further depicted in *Figure* 2.3.

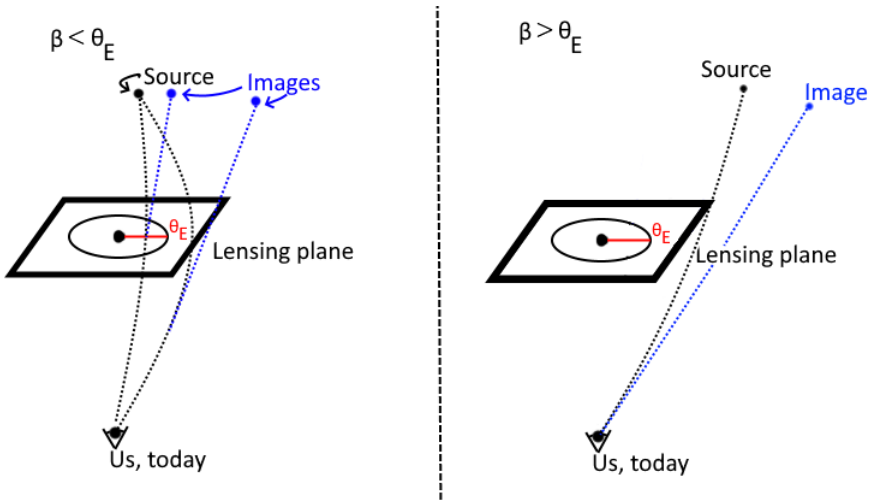

Figure 2.3: Having $\beta > \theta_E$ in the SIS model gives us a deflection rather than multiple images. On the other hand, $\beta < \theta_E$ gives us two images as desired. We must thus enforce this constraint.

Restricting to the case $\beta < \theta_E$, solving for $\vec{x}$ and subsequently rescaling back to our original coordinates now gives us the image positions

$$\theta_E \vec{\theta}(\vec{\beta}) = \vec{\beta} \pm \theta_E \frac{\vec{\beta}}{||\vec{\beta}||}. \tag{2.41}$$

Inserting (2.41) into (2.34) additionally gives us an analytic expression for the time delay in terms of purely the source position, namely

$$\boxed{\Delta t_{ab}(\vec{\beta}) = -8\pi \left(\frac{\sigma_v}{c}\right)^2 \frac{\chi_l}{c}(\|\vec{\beta}\|).} \tag{2.42}$$

2.2.2 Elliptical lens profiles

An elliptical model (SPEMD), defined as

$$\kappa(x,y) = \left[\frac{x^2 + y^2/\cos^2\beta + s^2}{E^2}\right]^{\eta/2-1} \tag{2.43}$$

by [24] will retain its deflection angle terms. Herein, the potential is acquired as $\nabla^2\psi(\vec{\theta}) = 2\kappa(\vec{\theta})$, as we are immediately given the convergence, which is the projected mass density of the lens. In this expression, $\cos\beta$ is the axis ratio of the ellipse, s is the core radius, E is some normalization factor which depends on the velocity dispersion, and η is the power-law factor which should be 1 in the isothermal case. By, again, making a few assumptions about the values some of these factors take, we can visualize $\kappa(x,y)$:

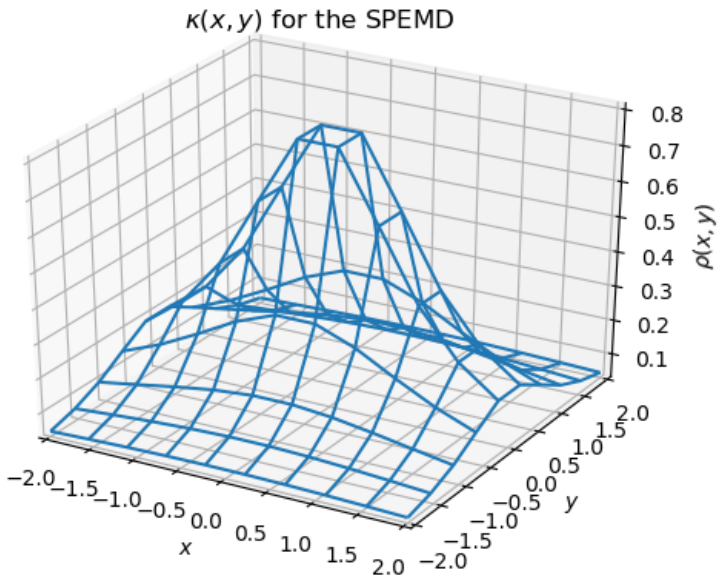

Figure 2.4: A depiction of $\kappa(x,y)$ for the SPEMD model for which we assumed $\eta = 1$, $E = 1$ and $\cos^2\beta = 0.5$. Note that the presence of the core radius s gets rid of the singularity that we saw in the SIS.

As opposed to the spherical case, which could be readily solved analytically, the elliptical model is unsolvable without Taylor expansion, even if we reduce it to the singular isothermal ellipse (SIE) by setting $\eta = 1, s = 0$. As such, we will henceforth stick to the simpler spherical model. It is notable that one can perturb (2.43) around the SIS.

2.3 Weak lensing

In describing weak lensing, one must make amends with the fact that there is no longer a clearly defined position for any one powerful lens, but rather a stack of many weaker lenses that lead to a net distortion of the final image.

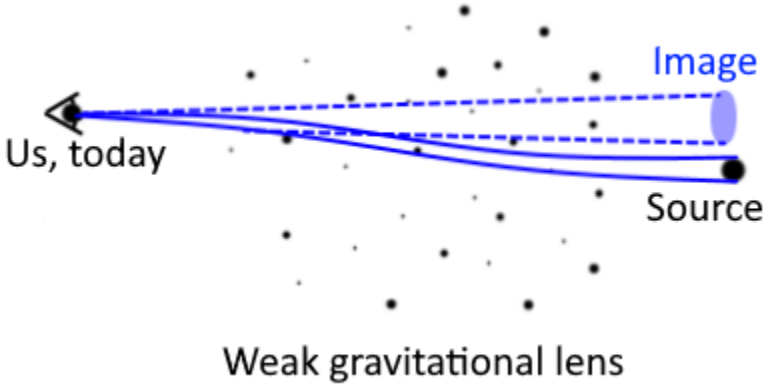

Figure 2.5: In weak gravitational lensing, observed effects are the result of many weaker gravitational lenses affecting the photon paths as opposed to a single strong lens. This leads to a net distortion of the observed image.

Due to this feature, one loses the analytic nature of the original theory, but instead gains knowledge on features such as average densities in entire regions of the celestial sphere, and their corresponding correlators. Indeed, we have succeeded in obtaining mass estimates for a number of clusters by merely adding up, more specifically statistically averaging over many small distortions. Thankfully, the theory behind this effect is well-understood, and most of this section is based on [22], wherein it is described.

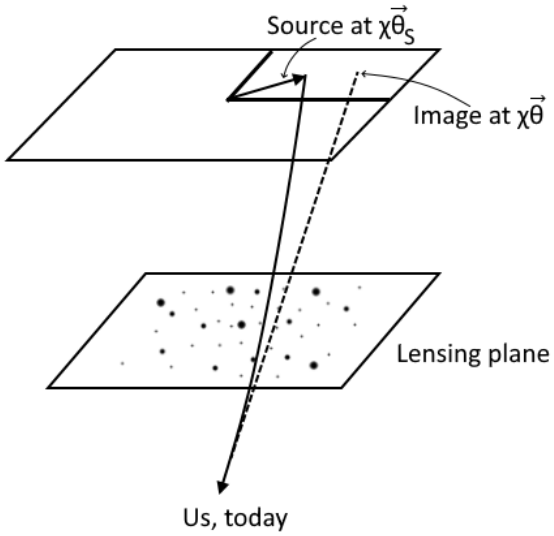

Figure 2.6: A depiction of the weak lensing scenario explained in (2.44). Light from a source at transverse coordinates $\chi\vec{\theta}_S$ is deflected to create an apparent image at transverse coordinates $\chi\vec{\theta}$.

Consider a photon at a position $\vec{x}$ from a distant source that passes through some overdense region in the sky. Its radial, or line-of-sight distance will be given by $x_3 = \chi$, whereas its transverse components will be given by $\vec{\theta}\chi$. Its path is affected by the density fluctuations, and it is subsequently observed by us as at position $\vec{\theta}$ as some intensity $I_{obs}(\vec{\theta})$. However, its true position is $\vec{\theta}_s$, and

$$I_{obs}(\vec{\theta}) = I_{true}(\vec{\theta}_s). \tag{2.44}$$

In order to parse the deflections of said photon, we will want to consider the geodesic equation. However, before doing so, we must account for the effects of overdensities on the metric. Indeed, our FLRW metric does not suffice in describing the perturbed spacetime that we find in the context of weak lensing. To this end, we define the perturbed diagonal metric

$$\begin{aligned} g_{00}(\vec{x}, t) &= -1 - 2\Psi(\vec{x}, t), \\ g_{ij}(\vec{x}, t) &= a^2(t)\delta_{ij}(1 + 2\Phi(\vec{x}, t)), \end{aligned} \tag{2.45}$$

where Φ, Ψ are Bardeen potentials. We can now consider the spatial components of the geodesic equation

$$\frac{d^2x^i}{d\lambda^2} = -\Gamma^i_{\alpha\beta}\frac{dx^\alpha}{d\lambda}\frac{dx^\beta}{d\lambda}, \tag{2.46}$$

where λ is some affine parameter. We want to express the affine parameter in terms of physical variables, to which end we use

$$\frac{d\chi}{d\lambda} = \frac{d\chi}{dt}\frac{dt}{d\lambda} = -\frac{1}{a(t)}p(1 - \Psi), \tag{2.47}$$

where $p^2 \equiv g_{\mu\nu}P^\mu P^\nu$, and P^μ, P^ν are photon four-momenta. By inserting this in (2.46), considering only the transverse components, assuming no anisotropic stress such that $\Phi = \Psi$, and assuming θ to be small, we find that

$$\frac{d^2}{d\chi^2}\left(\chi\theta^i\right) = 2\Phi_{,i}, \tag{2.48}$$

where the comma in $\Phi_{,i}$ indicates a spatial derivative. We can twice-integrate this expression to acquire a very general lens equation for the weak lensing case, namely

$$\beta^i = \frac{2}{\chi_s}\int_0^{\chi_s} d\chi'' \int_0^{\chi''} d\chi' \Phi_{,i}(\vec{x}(\chi')) + C. \tag{2.49}$$

We can note that the constant of integration C is, in fact, the observed image angle θ^i. We can additionally change the order of integration with the $d\chi''$ integral ranging from χ' to χ_s, as the two integral bounds combined restrict us to the region $\chi' < \chi'' < \chi_s$. Doing so makes one of the two integrals trivial, and we acquire the desired weak lensing equation

$$\boxed{\beta^i - \theta^i = 2\int_0^{\chi_s} d\chi' \Phi_{,i}(\vec{x}(\chi'))\left(1 - \frac{\chi'}{\chi_s}\right).} \tag{2.50}$$

We observe that we are integrating along our line-of-sight to the source, taking into consideration any overdensities along the way by means of the potential $\Phi(\vec{x})$, which is exactly the summation of many small distortions that we mentioned at the beginning of this section. It is typical to now define the transformation matrix

$$A_{ij} \equiv \frac{\partial\theta^i_s}{\partial\theta^j} \equiv \begin{pmatrix} 1 - \kappa - \gamma_1 & -\gamma_2 \\ -\gamma_2 & 1 - \kappa + \gamma_1 \end{pmatrix}, \tag{2.51}$$

which has several components that quantify the various effects of the weak lensing potential. The convergence κ encodes magnification effects, whereas the two components γ_1 and γ_2 encode shear effects. However, we will not need these components for our purposes, instead using (2.50) as our starting point for the weak lensing contaminant that we consider in section 6.

3 Phenomenological Model

The dark energy model that we consider will exhibit spatial correlations, unlike typical ΛCDM. In this chapter, we will describe how these correlations will appear in the energy density fields and their corresponding two-point functions. We can subsequently start considering how this carries through into physical observables.

In this description, we denote the dark energy density by the quantum mechanical operator $\hat{\rho}_Q(t, \vec{x})$, making it a function of spacetime as a whole. As a more natural choice of variables, we opt to use the redshift and unit angle on the celestial sphere instead, which is to say that we have $\hat{\rho}_Q(z, \hat{e})$. We take an ensemble average over the angular component, giving us an equal-time spacelike hypersurface, to define $\langle\hat{\rho}_Q\rangle(z)$. The potential origins of these fluctuations are detailed in [19].

As observed when taking the ensemble average, the one-point function of this density simply gets rid of any angular dependence. However, the angular dependence of the two-point function $\langle\hat{\rho}_Q(z, \hat{e}_A)\hat{\rho}_Q(z, \hat{e}_B)\rangle$ can be parametrized by a function $s_i(\|\hat{e}_A - \hat{e}_B\|)$, giving the following relation:

$$\langle\hat{\rho}_Q(z, \hat{e}_A)\hat{\rho}_Q(z, \hat{e}_B)\rangle = \langle\hat{\rho}_Q\rangle^2(z)s(\|\hat{e}_A - \hat{e}_B\|). \tag{3.1}$$

Note that we assume both $\hat{\rho}_Q$ to be at equal time. In practice, this will not always be the case, as we will be considering deep surveys and thus objects at considerably further distances. The corresponding expression for the unequal time correlator will be further detailed in section 4, specifically (4.17). One can assume several realizations of $\hat{\rho}_Q$, such as $\hat{\rho}_Q \propto \hat{\varphi}^2$ or $\hat{\rho}_Q \propto \hat{\varphi}$, leading to rather different s-functions. Herein, $\hat{\varphi}$ is a Gaussian quantum field as described in the aforementioned papers. Another notable feature is that, due to homogeneity and isotropy, only the norm of the difference between the angles matters for the s-function.

In this paper, we will assume that $\hat{\rho}_Q \propto \hat{\varphi}^2$, where $\langle\hat{\varphi}\rangle = 0$. That is to say that there is a zero vacuum expectation value, and our two-point function becomes

$$\begin{aligned}\langle\hat{\rho}_Q(z, \hat{e}_A)\hat{\rho}_Q(z, \hat{e}_B)\rangle &= \langle\hat{\varphi}^2(z, \hat{e}_A)\hat{\varphi}^2(z, \hat{e}_B)\rangle \\ &= \langle\hat{\varphi}^2\rangle^2(z) + 2\langle\hat{\varphi}(z, \hat{e}_A)\hat{\varphi}(z, \hat{e}_B)\rangle^2.\end{aligned} \tag{3.2}$$

When two fields are infinitely far apart so that $\|\hat{e}_A - \hat{e}_B\| \to \infty$, they should become completely uncorrelated and we should only retain $\langle\hat{\varphi}^2\rangle^2(z)$. However, when two fields coincide so that $\|\hat{e}_A - \hat{e}_B\| \to 0$, they should become fully correlated and we will have $2\langle\hat{\varphi}(z, \hat{e}_A)\hat{\varphi}(z, \hat{e}_B)\rangle^2 \to 2\langle\hat{\varphi}^2\rangle^2(z)$. We thus need the s-function to take up the value 1 at large distances, and climb up to 3 as the fields get closer together. We define said function as follows:

$$s(r) = \begin{cases} 3 - 2(\frac{r}{r_0})^{n_{DE}}, & r \leq r_0, \\ 1, & r > r_0. \end{cases} \tag{3.3}$$

We thus have a power law with a slope n_{DE}, which is the spectral index. This function also utilizes a characteristic length scale r_0, which turns out to be related to the comoving Hubble radius at inflation in the specific realization considered in this thesis. Both the spectral index and the characteristic length scale and their corresponding values will be physically motivated further in section 9.

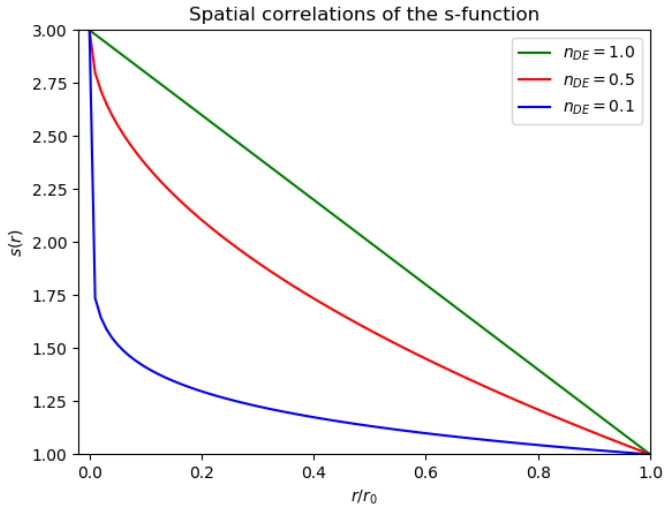

Figure 3.1: The function $s(r)$ plotted as a function of r/r_0 for various spectral indices n_{DE}. Note that the only difference between the three cases is the slope.

We note that our newly-introduced dark energy density operator will change the form of the Friedmann equation (2.10). Namely, we now have an operator equation that looks like

$$3M_p^2\hat{H}^2(z,\hat{n}) = \rho_C(z)\hat{I} + \hat{\rho}_Q(z,\hat{n}), \tag{3.4}$$

with $M_p = 2.435\times10^{18}$ GeV/c^2 the reduced Planck mass, ρ_C the classical matter densities and $\hat{I}$ the identity operator. In the next chapter, we will derive how this affects observables- in particular time delays in strong lenses.

As mentioned before, there are several realizations of this kind of model with various proportionalities for $\hat{\rho}_Q$. E.g. $\hat{\rho}_Q \propto \hat{\varphi}^4$ is not out of the question. However, changing the proportionality of $\hat{\rho}_Q$ to $\hat{\varphi}$ also changes the form of the s-function. In particular, we can derive that when $\hat{\rho}_Q \propto \hat{\varphi}^2$, the s-function appears as

$$s(r) = \begin{cases} \tilde{\sigma}_Q^2\left[1-\left(\frac{r}{r_0}\right)^{n_{DE}}\right]+1, & r \le r_0, \\ 1, & r > r_0, \end{cases} \tag{3.5}$$

where $\tilde{\sigma}_Q^2 = \frac{\sigma_Q^2}{\langle\hat{\rho}_Q\rangle^2}$, with σ_Q^2 the local variance of the energy density field $\hat{\rho}_Q$. Note that we recover (3.3) when we take $\tilde{\sigma}_Q^2 = 2$.

4 Dressed physical observables

In this chapter, we will derive how the dark energy fluctuations within this phenomenological model will affect time delays from strong lenses. In order to do this, let us consider the semi-classical approximation for (3.4), noting that $\rho_{tot} = \rho_c + \langle\rho_Q\rangle$. The angular brackets $\langle\dots\rangle$ now denote an ensemble average. The quantum mechanical fluctuations enter in the semi-classical approximation by means of a term $\delta\rho_Q(z,\hat{n})$ – which is no longer an operator – giving us

$$\frac{\delta\rho_Q(z,\hat{n})}{\rho_{tot}(z)} = \frac{\rho_Q(z,\hat{n}) - \langle\rho_Q\rangle(z)}{\rho_{tot}(z)}. \tag{4.1}$$

Combining this with (3.4), we can acquire an expression for $H^{-1}(z,\hat{n})$ which is dressed by fluctuations up to first order in $\delta\rho_Q(z,\hat{n})$ by Taylor expanding it:

$$H^{-1}(z,\hat{n}) \approx \bar{H}^{-1}(z)\left[1 + \frac{\delta\rho_Q(z,\hat{n})}{\rho_{tot}(z)}\right]^{-1/2}. \tag{4.2}$$

We can then define the bare comoving distance $\bar{\chi} := c\int_0^z \frac{dz'}{\bar{H}(z')}$, and expand the integral in terms of the fluctuation term $\omega_Q(z,\hat{n}) := \frac{\delta\rho_Q(z,\hat{n})}{\rho_{tot}(z)}$ to acquire corrections:

$$\delta\chi_l^{(1)} = -\frac{c}{2}\int_0^{z_l}\frac{dz}{\bar{H}(z)}\omega_Q, \tag{4.3}$$

$$\delta\chi_l^{(2)} = \frac{3c}{8}\int_0^{z_l}\frac{dz}{\bar{H}(z)}\omega_Q^2. \tag{4.4}$$

Performing this expansion with the comoving distance gives us an expression dressed by the dark energy fluctuations

$$\langle\hat{\chi}\rangle(z) = \int_0^z \frac{dz'}{\bar{H}(z')}\left(1 - \frac{1}{2}\omega_Q + \frac{3}{8}\omega_Q^2\right). \tag{4.5}$$

By definition, $\langle\omega_Q\rangle(z) = 0$, so we will only retain

$$\langle\hat{\chi}\rangle(z) = \int_0^z \frac{dz'}{\bar{H}(z)}\left(1 + \frac{3}{8}\frac{\langle\hat{\rho}_Q(z',\hat{n})^2\rangle - \langle\hat{\rho}_Q(z')\rangle^2}{\rho_{tot}^2(z')}\right). \tag{4.6}$$

We can now rewrite this in terms of the phenomenological s-function (3.3). This gives us the desired expression

$$\langle\hat{\chi}\rangle(z) = \int_0^z \frac{dz'}{\bar{H}(z)}\left(1 + \frac{3}{8}\Omega_Q(z')(s(0)-1)\right). \tag{4.7}$$

Note that we defined $\Omega_Q(z) \equiv \frac{\langle\rho_Q\rangle(z)}{\rho_{tot}(z)}$. For the time delay (2.42), things are rather more involved due to the presence of several comoving distances (the additional terms that appear out of β are further detailed in section 5)

$$\Delta t(\vec{\beta}) = -8\pi\left(\frac{\sigma_v}{c}\right)^2\frac{\chi_l}{c}\beta \to -32\pi^2\left(\frac{\sigma_v}{c}\right)^4\frac{\chi_l}{c}\left(1 - \frac{\chi_l}{\chi_s}\right). \tag{4.8}$$

4.1 Two-point function

In this section, we will consider the two-point function of (4.8) by using the same methodology as for $\chi(z)$. We start from the general expression

$$\langle\Delta t_a(\vec{\beta}_a)\Delta t_b(\vec{\beta}_b)\rangle = 64\pi^2\left(\frac{\sigma_{v,a}}{c}\right)^2\left(\frac{\sigma_{v,b}}{c}\right)^2\left\langle\frac{\chi_{l,a}}{c}\beta_a\frac{\chi_{l,b}}{c}\beta_b\right\rangle$$

$$\to 4(4\pi)^4 \left(\frac{\sigma_{v,a}}{c}\right)^4 \left(\frac{\sigma_{v,b}}{c}\right)^4 \left\langle \frac{\chi_{l,a}}{c}\left(1-\frac{\chi_{l,a}}{\chi_{s,a}}\right)\frac{\chi_{l,b}}{c}\left(1-\frac{\chi_{l,b}}{\chi_{s,b}}\right)\right\rangle. \tag{4.9}$$

We will now Taylor expand the full ensemble average, going up to second order in χ. To make the expression somewhat compact, let us first define

$$\alpha^{(1)}(z) = -\frac{c}{2}\frac{\int_0^z dz' \bar{H}^{-1}(z')\omega_Q(z',\hat{e})}{\int_0^z \frac{dz'}{\bar{H}(z')}}, \tag{4.10}$$

$$\alpha^{(2)}(z) = \frac{3c}{8}\frac{\int_0^z dz' \bar{H}^{-1}(z')\omega_Q^2(z',\hat{e})}{\int_0^z \frac{dz'}{\bar{H}(z')}}. \tag{4.11}$$

We can now write the expansion of (9.37) in terms of these functions, giving us the following equation up to second order in $\delta\chi$:

$$\begin{aligned}\langle \dots \rangle \approx{}& \frac{\bar{\chi}_{l(a)}}{c}\left(1-\frac{\bar{\chi}_{l(a)}}{\bar{\chi}_{s(a)}}\right)\frac{\bar{\chi}_{l(b)}}{c}\left(1-\frac{\bar{\chi}_{l(b)}}{\bar{\chi}_{s(b)}}\right)\\
&+\frac{\bar{\chi}_{l(a)}}{c}\frac{\bar{\chi}_{l(b)}}{c}\left\{\left(1-\frac{\bar{\chi}_{l(a)}}{\bar{\chi}_{s(a)}}\right)\left[\langle\alpha^{(2)}_{l(b)}\rangle - \frac{\bar{\chi}_{l(b)}}{\bar{\chi}_{s(b)}}\langle 2\alpha^{(2)}_{l(b)} - \alpha^{(2)}_{s(b)} + (\alpha^{(1)}_{l(b)} - \alpha^{(1)}_{s(b)})^2\rangle\right] + (a \longleftrightarrow b)[a \longleftrightarrow b]\right\}\\
&+\frac{\bar{\chi}_{l(a)}}{c}\frac{\bar{\chi}_{l(b)}}{c}\left[\left(1-2\frac{\bar{\chi}_{l(a)}}{\bar{\chi}_{s(a)}}\right)\left(1-2\frac{\bar{\chi}_{l(b)}}{\bar{\chi}_{s(b)}}\right)\langle\alpha^{(1)}_{l(a)}\alpha^{(1)}_{l(b)}\rangle + \frac{\bar{\chi}_{l(a)}}{\bar{\chi}_{s(a)}}\frac{\bar{\chi}_{l(b)}}{\bar{\chi}_{s(b)}}\langle\alpha^{(1)}_{s(a)}\alpha^{(1)}_{s(b)}\rangle\right]\\
&+\frac{\bar{\chi}_{l(a)}}{c}\frac{\bar{\chi}_{l(b)}}{c}\left[\left(1-2\frac{\bar{\chi}_{l(a)}}{\bar{\chi}_{s(a)}}\right)\frac{\bar{\chi}_{l(b)}}{\bar{\chi}_{s(b)}}\langle\alpha^{(1)}_{l(a)}\alpha^{(1)}_{s(b)}\rangle + \left(1-2\frac{\bar{\chi}_{l(a)}}{\bar{\chi}_{s(a)}}\right)\frac{\bar{\chi}_{l(a)}}{\bar{\chi}_{s(a)}}\langle\alpha^{(1)}_{l(b)}\alpha^{(1)}_{s(a)}\rangle\right].\end{aligned} \tag{4.12}$$

In this full correlator, we acquire several different individual correlators, some of which are more trivial to calculate than others. We will write all of them in terms of the s-function (3.3) and ω_Q as follows:

$$\langle\alpha^{(2)}\rangle = \frac{3}{8}(s(0)-1)\frac{\int_0^z \frac{dz'}{\bar{H}(z')}\Omega_Q^2(z')}{\int_0^z \frac{dz'}{\bar{H}(z')}}, \tag{4.13}$$

$$\langle(\alpha^{(1)})^2\rangle = \frac{1}{4}\frac{\int_0^z \frac{dz'}{\bar{H}(z')}\int_0^z \frac{dz''}{\bar{H}(z'')}\langle\omega_Q(z',\hat{e}_a)\omega_Q(z'',\hat{e}_a)\rangle}{\int_0^z \frac{dz'}{\bar{H}(z')}\int_0^z \frac{dz''}{\bar{H}(z'')}}, \tag{4.14}$$

$$\langle\alpha_{l(i)}\alpha_{s(i)}\rangle = \frac{1}{4}\frac{\int_0^{z_{l(a)}} \frac{dz'}{\bar{H}(z')}\int_0^{z_{s(a)}} \frac{dz''}{\bar{H}(z'')}\langle\omega_Q(z',\hat{e}_i)\omega_Q(z'',\hat{e}_i)\rangle}{\int_0^{z_{l(a)}} \frac{dz'}{\bar{H}(z')}\int_0^{z_{s(a)}} \frac{dz''}{\bar{H}(z'')}}, \tag{4.15}$$

$$\langle\alpha_{l(a)}\alpha_{s(b)}\rangle = \frac{1}{4}\frac{\int_0^{z_{l(a)}} \frac{dz'}{\bar{H}(z')}\int_0^{z_{s(b)}} \frac{dz''}{\bar{H}(z'')}\langle\omega_Q(z',\hat{e}_a)\omega_Q(z'',\hat{e}_b)\rangle}{\int_0^{z_{l(a)}} \frac{dz'}{\bar{H}(z')}\int_0^{z_{s(b)}} \frac{dz''}{\bar{H}(z'')}}. \tag{4.16}$$

The difference between the final two correlators, in particular, might seem redundant. However, it is crucial to note that a difference in angular position between the two observables will carry through into the s-function, giving us vastly different expressions in the end. We note that we can readily express and calculate $\langle\alpha^{(2)}\rangle$ due to it being at a single redshift z. However, the other expressions require an unequal time correlator

$$\begin{aligned}\langle\omega(z_1,\hat{e}_a)\omega(z_2,\hat{e}_b)\rangle ={}& \frac{H_0^4}{\bar{H}^2(z_1)\bar{H}^2(z_2)}\Omega_Q^2(0)s(\|\bar{\chi}(z_1)\hat{e}_a - \bar{\chi}(z_2)\hat{e}_b\|),\\
&\times\left[1-\frac{3(\Omega_M+1/\alpha)}{(\alpha+1)(\Omega_\Lambda-1/\alpha)}\left(\int_0^{z_1}\frac{dz'}{1+z'}\frac{H_0}{\bar{H}(z')}+\int_0^{z_2}\frac{dz''}{1+z''}\frac{H_0}{\bar{H}(z'')}\right)\right] - \Omega_Q(z_1)\Omega_Q(z_2),\end{aligned} \tag{4.17}$$

of which the derivation is further detailed in Appendix C. This expression has already been adjusted to accommodate the model that we will further detail in section 9, hence it including the model constant α.

5 Angular power spectrum

In order to create a link to the observations we make of the sky, it is fruitful to express predicted theoretical effects in terms of spherical harmonics. This allows one to capture wide-angle effects, and is quite a natural choice given our observed celestial sphere. To this end, we will use the angular power spectrum C_ℓ, where ℓ gives the mode index [25] and $Y_{\ell m}$ are the corresponding spherical harmonics.

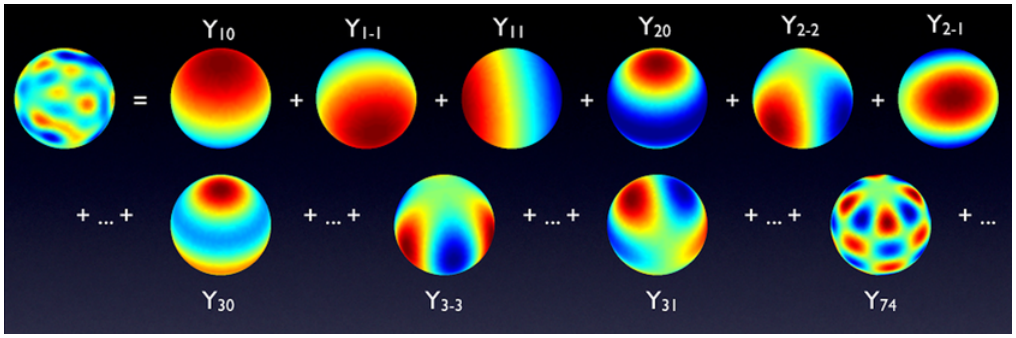

Figure 5.1: We can decompose correlators into spherical harmonics to better represent observed data [26].

Decomposing the time delay in terms of these spherical harmonics gives us

$$\Delta t(\hat{e}, \{P_i\}) = \sum_{\ell=0}^{\infty} \sum_{m=-\ell}^{l} a_{\ell m}(\{P_i\}) Y_{\ell m}(\hat{e}), \tag{5.1}$$

where we introduced $\hat{e}$, the position of the lens in the sky, and $\{P_i\} = \{\hat{n} \perp \hat{e}, \beta, \chi_l, \chi_s, \sigma_v\}$, which encodes all other variables. Note that we parametrize the separation of the source from the center of the lens by means of vector $\hat{n}$, which is perpendicular to the lens position $\hat{e}$ and indicates the direction- β then denotes the corresponding magnitude. However, we can parametrize the direction $\hat{n}$, which lies on the plane orthogonal to $\hat{e}$, with a single angle ψ. $a_{\ell m}$ are the coefficients of the modes, and have the additional property that they are stochastic variables. This allows us to take an ensemble average over them. Inverting (5.1), we find

$$a_{\ell m}(\{P_i\}) = \int d^2\hat{e} Y^*_{\ell m}(\hat{e}) \Delta t(\hat{e}, \{P_i\}), \tag{5.2}$$

at which point we can take the aforementioned ensemble average between two strong gravitational lens systems

$$\langle a_{\ell m}(\{P_i\}) a^*_{\ell' m'}(\{P'_i\})\rangle = C_\ell(\{P_i\}, \{P'_i\}) \delta_{\ell\ell'} \delta_{mm'}, \tag{5.3}$$

where δ denotes the Kronecker delta. It is notable that this average concerns an ensemble of universes. However, we only have a single observable universe that we can sample over, yielding a so-called cosmic variance. Assumed statistical isotropy further allows us to average over the individual m-modes, as there is no useful information in them. Note that these run from $-\ell$ to ℓ, giving $2\ell + 1$ of them. Therefore,

$$C_\ell(\{P_i\}, \{P'_i\}) = \frac{1}{2\ell+1} \sum_{m=-\ell}^{\ell} \langle a_{\ell m}(\{P_i\}) a^*_{\ell m}(\{P'_i\})\rangle \tag{5.4}$$

$$= \frac{1}{2\ell+1} \sum_{m=-\ell}^{\ell} \int d^2\hat{e} \int d^2\hat{e}' Y^*_{\ell m}(\hat{e}) Y_{\ell m}(\hat{e}') \langle \Delta t(\hat{e}, \{P_i\}) \Delta t(\hat{e}', \{P'_i\})\rangle. \tag{5.5}$$

We can now use the orthogonality relation

$$P_\ell(\hat{a} \cdot \hat{b}) \equiv \frac{4\pi}{2\ell+1} \sum_{m=-\ell}^{\ell} Y^*_{\ell m}(\hat{a}) Y_{\ell m}(\hat{b}) \tag{5.6}$$

to rewrite (5.5) as

$$C_\ell(\{P_i\},\{P_i'\}) = \frac{1}{4\pi}\int d^2\hat{e}\int d^2\hat{e}' P_\ell(\hat{e}\cdot\hat{e}')\langle\Delta t(\hat{e},\{P_i\})\Delta t(\hat{e}',\{P_i'\})\rangle. \tag{5.7}$$

It is beneficial to now consider the distributions of P_i. Although some of these distributions can be determined logically, others must be considered numerically. For ψ, we can assume a uniform distribution on $[0,2\pi]$ due to statistical isotropy. For $\beta = ||\vec{\beta}||$, we note that we are restricted by the condition $\beta < \theta_E$. As detailed in section 2, having a β larger than this would imply a deflection of the light rather than the appearance of multiple images, so we take this as an upper limit for a uniform distribution. Notably, this is what introduces the additional comoving distances mentioned in (4.8). Finally, we will acquire distributions for χ_l, χ_s and σ_v by means of a mock dataset which will be detailed in section 7. We thus have the following distributions:

ψ	$[0,2\pi]$
β	$[0, 4\pi(1-\frac{\chi_l}{\chi_s})(\frac{\sigma_v}{c})^2]$
χ_l, χ_s, σ_v	Mock data

We can further simplify (5.7) by noting that the angular dependence of the correlator $\Delta t(\hat{e},\{P_i\})\Delta t(\hat{e}',\{P_i'\})$ only appears in the relative angle: as the background is isotropic, the exact positions are irrelevant. However, there is a catch: this is only true when we do not consider the perturbed ΛCDM setup that we have for the weak lensing correlator. Details of this setup will follow in section 6. However, one must first integrate over ψ before one can make this statement in this section. Having noted this key difference, we will replace $\hat{e}\cdot\hat{e}' = \cos(\theta) = \mu$, giving us

$$C_\ell(\{P_i\},\{P_i'\}) = 2\pi\int_{-1}^{1} d\mu\langle\Delta t(\{P_i\})\Delta t(\{P_i'\})\rangle(\mu)P_l(\mu). \tag{5.8}$$

Integrating over ψ and β using the given distributions, integrating over χ_l, χ_s and σ_v with probability densities P_i derived from the mock data and combining (9.37) and (5.8) nets us the desired expression for the C_ℓ:

$$C_\ell = \frac{16}{9}(4\pi)^4\iiint d\chi_{l,a}d\chi_{s,a}d\sigma_{v,a}P_l(\chi_{l,a})P_s(\chi_{s,a})P_\sigma(\sigma_{v,a})\iiint d\chi_{l,b}d\chi_{s,b}d\sigma_{v,b}P_l(\chi_{l,b})P_s(\chi_{s,b})P_\sigma(\sigma_{v,b})$$
$$\times\left(\frac{\sigma_{v,a}}{c}\right)^4\left(\frac{\sigma_{v,b}}{c}\right)^4\frac{1}{4\pi}\int d^2\hat{e}_a\int d^2\hat{e}_b P_\ell(\hat{e}_a\cdot\hat{e}_b)\left\langle\frac{\chi_{l,a}(\hat{e}_a)}{c}\left[1-\frac{\chi_{l,a}(\hat{e}_a)}{\chi_{s,a}(\hat{e}_a)}\right]\frac{\chi_{l,b}(\hat{e}_b)}{c}\left[1-\frac{\chi_{l,b}(\hat{e}_b)}{\chi_{s,b}(\hat{e}_b)}\right]\right\rangle. \tag{5.9}$$

We note that we get a power spectrum in units of time squared, which is expected as we are computing correlators of time delays. Herein, we recall that $\langle\dots\rangle$ can be expanded as (4.12). We additionally recall that said expansion leads to the presence of terms $\langle\omega(z_1,\hat{e}_a)\omega(z_2,\hat{e}_b)\rangle$ which give rise to the s-function $s(\|\bar{\chi}(z_1)\hat{e}_a - \bar{\chi}(z_2)\hat{e}_b\|)$. In order to calculate these, one needs to solve integrals of the form

$$\frac{1}{4\pi}\int d^2\hat{e}_a\int d^2\hat{e}_b P_\ell(\hat{e}_a\cdot\hat{e}_b)s(\|\bar{\chi}(z_1)\hat{e}_a - \bar{\chi}(z_2)\hat{e}_b\|). \tag{5.10}$$

As the s-function is defined piecewise, the integral will be too. Namely, we acquire the following:
For $r_0 > \bar{\chi}_1 + \chi_2$ (Case I), we get

$$12\pi\delta_{\ell 0} - 4\pi\left(\frac{\bar{\chi}_1^2+\bar{\chi}_2^2}{r_0^2}\right)^{\frac{n_{DE}}{2}}\frac{\sqrt{\pi}}{(2\mu_0(z_1,z_2))^\ell}\frac{\Gamma(\ell-\frac{n_{DE}}{2})}{\Gamma(\ell+\frac{3}{2})\Gamma(-\frac{n_{DE}}{2})}$$
$$\times\ {}_2F_1\left(\frac{\ell}{2}-\frac{n_{DE}}{4},\frac{1}{2}+\frac{\ell}{2}-\frac{n_{DE}}{4};\frac{3}{2}+\ell;\frac{1}{\mu_0^2(z_1,z_2)}\right), \tag{5.11}$$

for $r_0 < |\chi_1 - \chi_2|$ (Case II), we get $4\pi\delta_{\ell 0}$,
and for $|\chi_1 - \chi_2| < r_0 < \bar{\chi}_1 + \bar{\chi}_2$ (Case III), we get

$$4\pi\delta_{\ell 0} + 4\pi\frac{P_{\ell-1}(\nu_0) - P_{\ell+1}(\nu_0)}{2\ell+1} - 4\pi\left(\frac{\bar{\chi}_1^2 + \bar{\chi}_2^2}{r_0^2}\right)^{n_{DE}/2}\int_{\nu_0}^1 d\mu P_\ell(\mu)\left(1 - \frac{\mu}{\mu_0}\right)^{n_{DE}/2}. \tag{5.12}$$

Herein, we defined

$$\mu_0(z_1, z_2) = \frac{\bar{\chi}^2(z_1) + \bar{\chi}^2(z_2)}{2\chi(z_1)\chi(z_2)}, \quad \nu_0(z_1, z_2) = \frac{\bar{\chi}^2(z_1) + \bar{\chi}^2(z_2) - r_0^2}{2\chi(z_1)\chi(z_2)} \tag{5.13}$$

for ease of notation. These functions are bounded by definition as $\mu_0 \geq 0$ and $-1 < \nu_0 < 1$. Note that we already integrated over the relative angle $\mu = \hat{e}_a \cdot \hat{e}_b = \cos(\theta)$ in cases I and II. However, Case III contains a slightly more involved expression which we will write down explicitly:

$$\int_{\nu_0}^1 d\mu P_\ell(\mu)\left(1 - \frac{\mu}{\mu_0}\right)^{n_{DE}/2} = -\left(1 - \frac{\nu_0}{\mu_0}\right)^{\frac{n_{DE}}{2}}\sum_{k=0}^{\ell}\frac{(\ell+k)!}{(\ell-k)!(k!)^2}\frac{(\nu_0-1)^{k+1}}{(k+1)2^k}$$
$$\times \quad {}_2F_1\left(-\frac{n_{DE}}{2}, 1; k+2; \frac{1-\nu_0}{\mu_0-\nu_0}\right). \tag{5.14}$$

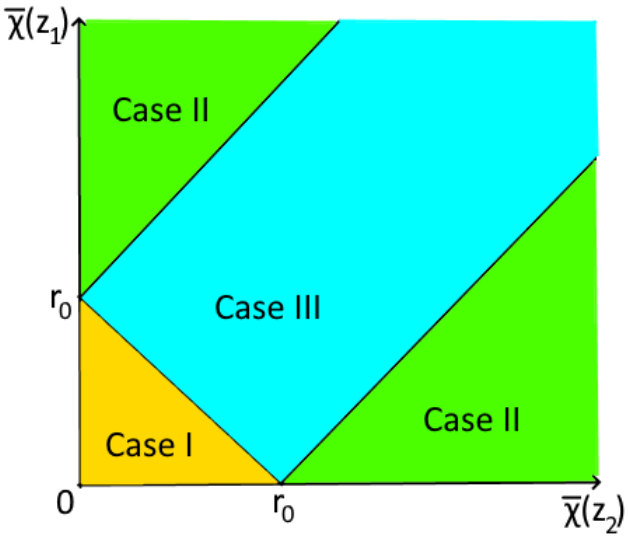

Figure 5.2: When solving the integrals in (5.10), we have to deal with three cases depending on how the values of $\bar{\chi}_1$ and $\bar{\chi}_2$ relate to r_0. Namely, case I: $r_0 > \bar{\chi}_1 + \chi_2$, case II: $r_0 < |\chi_1 - \chi_2|$ and case III: $|\chi_1 - \chi_2| < r_0 < \bar{\chi}_1 + \bar{\chi}_2$.

6 Weak lensing as a contaminant

One important feature of a measurable signal is a range of values that peaks above sources of noise. In practice, these sources of noise will act as a contaminant on top of the spatial correlations in dark energy, leading to fluctuations that are unrelated to the model that we are interested in. One such contaminant is the weak lensing effect. As we will be considering correlators of time delays corresponding to different regions of the sky, it is natural to assume that the influence of weak lensing will be felt differently as well. Notably, this weak lensing contribution should also be calculated within the context of our dark energy model. However, this goes beyond the scope of this thesis. As such, the weak lensing contaminant will be considered in a ΛCDM context.

To obtain the equation describing the weak lensing contaminant, we will start from the lens equation, now considering a linear combination of strong and weak lensing potentials:

$$\psi = \psi_{SL} + \psi_{WL}.$$

In doing so, we can separate the strong lensing and weak lensing contributions to the deflection angle and treat the problem perturbatively, truncating up to first order in ψ_{WL}. Solving this gives the following expression for the (two) deflected image positions:

$$\vec{\theta}_{\pm} \approx \vec{\theta}_{\pm}^{(SL)} + \vec{\theta}_{\pm}^{(WL)} \approx \frac{\vec{\beta}}{\theta_E}(1 \pm \frac{\theta_E}{||\vec{\beta}||})$$

$$+(1 \pm \frac{\theta_E}{||\vec{\beta}||})\vec{\nabla}_{\hat{n}}\psi_{WL}|_{\vec{\beta}} \mp \frac{\theta_E}{||\vec{\beta}||}\partial_{\hat{n}}\psi_{WL}|_{\vec{\beta}}\hat{n} + \theta_E(\frac{\theta_E}{||\vec{\beta}||} \pm 1)\vec{\nabla}\partial_{\hat{n}}\psi_{WL}|_{\vec{\beta}} - \frac{\theta_E^2}{||\vec{\beta}||}\partial_{\hat{n}}^2\psi_{WL}|_{\vec{\beta}}\hat{n}, \tag{6.1}$$

where we defined $\hat{n} := \frac{\vec{\beta}}{||\vec{\beta}||}$ and $n_i\partial_i := \partial_{\hat{n}}$. Using this, we can also derive an expression that includes a weak lensing contaminant for the time delay, which miraculously (See D) acquires the following elegant form:

$$\boxed{\Delta t(\vec{\beta}) = -8\pi(\frac{\sigma_v}{c})^2\frac{\chi_l}{c}(||\vec{\beta}|| + \partial_{\hat{n}}\psi_{WL}|_{\vec{\beta}}) + \mathcal{O}(\psi_{WL}^2).} \tag{6.2}$$

Herein, $\chi_l \equiv (1+z_l)D_l$ is the comoving distance in a flat FLRW universe. In order to link this to observable data, one must construct correlators for these time delays. Our correlator generally has the form

$$\langle \Delta t_a \Delta t_b \rangle = 64\pi^2(\frac{\sigma_{v,a}}{c})^2(\frac{\sigma_{v,b}}{c})^2 \left\langle \frac{\chi_{l,a}}{c}(||\vec{\beta}_a|| + \partial_{\hat{n}}^{(a)}\psi_{WL}|_{\vec{\beta}_a})\frac{\chi_{l,b}}{c}(||\vec{\beta}_b|| + \partial_{\hat{n}}^{(b)}\psi_{WL}|_{\vec{\beta}_b}) \right\rangle \tag{6.3}$$

when we consider two strong lenses labelled a and b. However, because we are considering the weak lensing component to be a contaminant on top of the dark energy fluctuations that enter χ_l, we will not take into account the effect of dark energy fluctuations on ψ_{WL}, and we can then separate the different correlators. In addition, we can immediately note that certain quantities, such as $||\vec{\beta}||\partial_{\hat{n}}\psi_{WL}|_{\vec{\beta}}$, will be uncorrelated. We can thus neglect these entirely. Our naive initial expression can thus be written in the following, more physically motivated manner:

$$\langle \Delta t_a \Delta t_b \rangle = 64\pi^2(\frac{\sigma_{v,a}}{c})^2(\frac{\sigma_{v,b}}{c})^2\frac{\langle \chi_{l,a}\chi_{l,b}\rangle}{c^2}(||\vec{\beta}_a||||\vec{\beta}_b|| + \langle \partial_{\hat{n}}^{(a)}\psi_{WL}|_{\vec{\beta}_a}\partial_{\hat{n}}^{(b)}\psi_{WL}|_{\vec{\beta}_b}\rangle). \tag{6.4}$$

One can now clearly see how the weak lensing potentials act as a contaminant on top of the effect of the dark energy fluctuations, which will dress the expression for $\langle \chi_{l,a}\chi_{l,b}\rangle$.

Although the form of this correlator is rather elegant, in part due to the expression for the time delay, the weak lensing correlator is quite non-trivial. We start from the typical expression that we derived at the end of *section* 2. We thus have the following general expression:

$$\langle \partial_{\hat{n}}^{(a)}\psi_{WL}|_{\vec{\beta}_a}\partial_{\hat{n}}^{(b)}\psi_{WL}|_{\vec{\beta}_b}\rangle = 4n_{A,i}n_{B,j}\int_0^{\chi_s^{(A)}} d\chi' \left(1 - \frac{\chi'}{\chi_s^{(A)}}\right)\int_0^{\chi_s^{(B)}} d\chi'' \left(1 - \frac{\chi''}{\chi_s^{(B)}}\right)\langle \Phi_{,i}^{(A)}\Phi_{,j}^{(B)}\rangle. \tag{6.5}$$

We subsequently Fourier transform these potentials, i.e.

$$\Phi(\eta,\vec{x}) = \int \frac{d^3k}{(2\pi)^3} e^{i\vec{k}\cdot\vec{x}}\tilde{\Phi}(\eta,\vec{k}). \tag{6.6}$$

This is also where the time-dependence of the potentials becomes relevant, as the two sources will be at two different redshifts, which can be rather high given modern surveys. This is to say that, generally,

$$\langle\tilde{\Phi}(\eta_0-\chi',\vec{k}')\tilde{\Phi}^*(\eta_0-\chi'',\vec{k}'')\rangle = (2\pi)^3\delta^{(3)}(\vec{k}'-\vec{k}'')P_\Phi(k',\eta_0-\chi',\eta_0-\chi''), \tag{6.7}$$

where η_0 denotes the conformal time today. We thus have a power spectrum with a time-dependence. In this work, we opted to expand the power spectrum in terms of potential growth functions $D_\Phi(\eta_0-\chi)$. We will therefore use

$$P_\Phi(k',\eta_0-\chi',\eta_0-\chi'') = D_\Phi(\eta_0-\chi')D_\Phi(\eta_0-\chi'')P_\Phi(k',\eta_0,\eta_0). \tag{6.8}$$

A more detailed derivation of this power spectrum and the form that it takes can be found in appendix D. Using the aforementioned Fourier transform and the generalized power spectrum, we can express the full weak lensing correlator as follows:

$$\langle\partial^{(A)}_{\hat{n}}\psi_{WL}|_{\vec{\beta}_A}\partial^{(B)}_{\hat{n}}\psi_{WL}|_{\vec{\beta}_B}\rangle = 4\left(\hat{n}_A\cdot\frac{\partial}{\partial\hat{e}_A}\right)\exp\left(\beta_a\hat{n}_a\cdot\frac{\partial}{\partial\hat{e}_A}\right)\left(\hat{n}_B\cdot\frac{\partial}{\partial\hat{e}_B}\right)\exp\left(\beta_B\hat{n}_B\cdot\frac{\partial}{\partial\hat{e}_B}\right)$$

$$\times\int_0^{\chi_s^{(A)}}d\chi'\left(\frac{1}{\chi'}-\frac{1}{\chi_s^{(A)}}\right)\int_0^{\chi_s^{(B)}}d\chi''\left(\frac{1}{\chi''}-\frac{1}{\chi_s^{(B)}}\right)\int\frac{d^3k}{(2\pi)^3}P_\Phi(k,\eta_0-\chi',\eta_0-\chi'')e^{i\vec{k}\cdot(\hat{e}_A\chi'-\hat{e}_B\chi'')}. \tag{6.9}$$

Note that we have an expression which contains all orders of β, making it fully general. We will find out that we require this, as integrating over a uniformly distributed β will cause lower-order contributions to vanish entirely.

The integral over k in (6.9) must now depend on the relative angle between the two systems, which is to say that we will acquire a result of the form $F(\hat{e}_A\cdot\hat{e}_B)$. We now use a plane wave expansion in spherical coordinates

$$e^{i\vec{k}\cdot\vec{r}} = \sum_0^\infty(2l+1)i^l j_l(kr)P_l(\hat{k}\cdot\hat{r}), \tag{6.10}$$

where j_l are spherical Bessel functions and P_l Legendre polynomials. This allows us to write the integral over k as follows

$$\int\frac{d^3k}{(2\pi)^3}P_\Phi(k,\eta_0-\chi',\eta_0-\chi'')e^{i\vec{k}\cdot(\hat{e}_A\chi'-\hat{e}_B\chi'')} = \int\frac{dk}{(2\pi)^3}k^2P_\Phi(k,\eta_0-\chi',\eta_0-\chi'')$$

$$\times\int d^2\hat{k}\sum_{l_A=0}^\infty\sum_{l_B=0}^\infty(2l_A+1)i^{l_A}(2l_B+1)(-i)^{l_B}j_{l_A}(k\chi')j_{l_B}(k\chi'')P_{l_A}(\hat{e}_A\cdot\hat{k})P_{l_B}(\hat{e}_B\cdot\hat{k}). \tag{6.11}$$

We can further rewrite this by using the following orthogonality relation

$$P_l(\hat{a}\cdot\hat{b}) \equiv \frac{4\pi}{2l+1}\sum_{n=-l}^{l}Y^*_{lm}(\hat{a})Y_{lm}(\hat{b}), \tag{6.12}$$

where Y_{lm} are spherical harmonics. Combining this with (6.11), we find that we can solve the angular integrals, only retaining the magnitude:

$$\int d^2\hat{k}P_{l_A}(\hat{e}_A\cdot\hat{k})P_{l_B}(\hat{e}_B\cdot\hat{k})$$

$$= \frac{4\pi}{2l_A+1}\frac{4\pi}{2l_B+1}\sum_{m_A=-l_A}^{l_A}\sum_{m_B=-l_B}^{l_B}\int d^2\hat{k}Y^*_{l_Am_A}(\hat{e}_A)Y_{l_Am_A}(\hat{k})Y^*_{l_Bm_B}(\hat{e}_B)Y_{l_Bm_B}(\hat{k})$$

$$= (\frac{4\pi}{2l+1})^2\sum_{m=-l}^{l}Y^*_{lm}(\hat{e}_A)Y_{lm}(\hat{e}_B) = \frac{4\pi}{2l+1}P_l(\hat{e}_A\cdot\hat{e}_B). \tag{6.13}$$

Subsequently, we can insert this into (6.11), which we then insert into the integral over k in (6.9) to acquire

$$\int\frac{d^3k}{(2\pi)^3}P_\Phi(k,\eta_0-\chi',\eta_0-\chi'')e^{i\vec{k}\cdot(\hat{e}_A\chi'-\hat{e}_B\chi'')}$$

$$= \int_0^\infty\frac{dk}{2\pi^2}k^2P_\Phi(k,\eta_0-\chi',\eta_0-\chi'')\sum_{L=1}^{\infty}(2L+1)j_L(k\chi')j_L(k\chi'')P_L(\hat{e}_A\cdot\hat{e}_B). \tag{6.14}$$

Note that this is, indeed, of the form $F(\hat{e}_A\cdot\hat{e}_B)$ that we expected. We start at $L=1$ as term $L=0$ does not contribute to the derivatives that we will inevitably get when considering terms that are of a higher order in β, and we identify

$$F(\hat{e}_A\cdot\hat{e}_B) = 4\sum_{L=1}^{\infty}P_L(\hat{e}_A\cdot\hat{e}_B)\int_0^{\chi_s^{(A)}}d\chi'\left(\frac{1}{\chi'}-\frac{1}{\chi_s^{(A)}}\right)\int_0^{\chi_s^{(B)}}d\chi''\left(\frac{1}{\chi''}-\frac{1}{\chi_s^{(B)}}\right)$$

$$\times\int_0^\infty\frac{dk}{2\pi^2}k^2P_\Phi(k,\eta_0-\chi',\eta_0-\chi'')(2L+1)j_L(k\chi')j_L(k\chi''). \tag{6.15}$$

We will now rewrite the correlator in terms of $F(\hat{e}_A\cdot\hat{e}_B)$. In doing so, we find that we acquire derivatives

$$F^{(n)}(\hat{e}_A\cdot\hat{e}_B) = \frac{\partial^nF(\hat{e}_A\cdot\hat{e}_B)}{\partial(\hat{e}_A\cdot\hat{e}_B)^n}. \tag{6.16}$$

The correlator then becomes

$$\langle\partial^{(A)}_{\hat{n}}\psi_{WL}|_{\vec{\beta}_A}\partial^{(B)}_{\hat{n}}\psi_{WL}|_{\vec{\beta}_B}\rangle = (\hat{n}_A\cdot\hat{n}_B)F^{(1)}(\hat{e}_A\cdot\hat{e}_B)+(\hat{n}_A\cdot\hat{e}_B)(\hat{n}_B\cdot\hat{e}_A)F^{(2)}(\hat{e}_A\cdot\hat{e}_B)$$

$$+(\beta_A\hat{n}_A\cdot\hat{e}_B+\beta_B\hat{n}_B\cdot\hat{e}_A)\cdot\Big[2(\hat{n}_A\cdot\hat{n}_B)F^{(2)}(\hat{e}_A\cdot\hat{e}_B)+(\hat{n}_A\cdot\hat{e}_B)(\hat{n}_B\cdot\hat{e}_A)F^{(3)}(\hat{e}_A\cdot\hat{e}_B)\Big]$$

$$+\beta_A\beta_B\cdot\Big[2(\hat{n}_A\cdot\hat{n}_B)^2F^{(2)}(\hat{e}_A\cdot\hat{e}_B)+(\hat{n}_A\cdot\hat{e}_B)(\hat{n}_B\cdot\hat{e}_A)F^{(3)}(\hat{e}_A\cdot\hat{e}_B)+(\hat{n}_A\cdot\hat{e}_B)^2(\hat{n}_B\cdot\hat{e}_A)^2F^{(4)}(\hat{e}_A\cdot\hat{e}_B)\Big]$$

$$+\ldots \tag{6.17}$$

Herein, we only retain the term on the third line, as integrating over $\hat{n}_A$ and $\hat{n}_B$ causes the other lower-order terms to vanish. We can therefore also omit the term $L=1$. The resulting expression is rather non-trivial as it involves several integrals of products of differentiated Legendre polynomials. In particular, the following integral which we denote $I(\ell,L)$ appears:

$$I(\ell,L) = \int_{-1}^{1}d\mu P_\ell(\mu)[2(\mu^2+1)P''_L(\mu)+4(\mu^3-\mu)P'''_L(\mu)+(1-\mu^2)^2P''''_L(\mu)]$$

$$= \begin{cases}4(L^2+L-3\ell^2-3\ell-2), & \text{if } L=\ell+2,\ell+4,\ell+6,\ell+8,\ldots\\ \frac{2\ell^2(\ell-1)^2}{2\ell+1}, & \text{if } L=l,\\ 0, & \text{otherwise.}\end{cases} \tag{6.18}$$

Note that we wrote everything in terms of the intermediate angle μ, analogously to the process detailed in *section* 5. Taking this, using (2.20) to write it in terms of overdensities and subsequently combining it with (6.8) nets us the angular power spectrum

$$C_\ell(\sigma_{v(a,b)},\chi_{l(a,b)},\chi_{s(a,b)}) = \frac{8}{9}(4\pi)^5\left(\frac{\sigma_{v(a)}}{c}\right)^4\left(\frac{\sigma_{v(b)}}{c}\right)^4\frac{\chi_{l(a)}}{c}\left(1-\frac{\chi_{l(a)}}{\chi_{s(a)}}\right)\frac{\chi_{l(b)}}{c}\left(1-\frac{\chi_{l(b)}}{\chi_{s(b)}}\right)$$
$$\times\left[2\delta_{\ell 0}+\int_0^\infty dk\frac{9\Omega_{m,0}^2}{8\pi^2k^2}\left(\frac{H_0}{c}\right)^4 P_{m,0}(k)\sum_{L=2}^{\infty}(2L+1)I(\ell,L)h_L(k;\chi_{s(a)})h_L(k;\chi_{s(b)})\right], \tag{6.19}$$

where we defined

$$h_L(k;\chi_s) = \int_0^{\chi_s} d\chi'\left(\frac{1}{\chi'}-\frac{1}{\chi_s}\right)j_L(k\chi')\frac{D_1(z(\chi'))}{a(z(\chi'))}. \tag{6.20}$$

We now want to integrate over any remaining variables. We will do this analogously to section 5, where we introduced probability distribution functions for the variables by means of a mock dataset, which will be detailed further in the following section. Introducing these integrals gives us the desired angular power spectrum

$$C_\ell = \frac{8}{9}(4\pi)^5\iiint d\chi_{l,a}d\chi_{s,a}d\sigma_{v,a}P_l(\chi_{l,a})P_s(\chi_{s,a})P_\sigma(\sigma_{v,a})\iiint d\chi_{l,b}d\chi_{s,b}d\sigma_{v,b}P_l(\chi_{l,b})P_s(\chi_{s,b})P_\sigma(\sigma_{v,b})$$
$$\times\left(\frac{\sigma_{v(a)}}{c}\right)^4\left(\frac{\sigma_{v(b)}}{c}\right)^4\frac{\chi_{l(a)}}{c}\left(1-\frac{\chi_{l(a)}}{\chi_{s(a)}}\right)\frac{\chi_{l(b)}}{c}\left(1-\frac{\chi_{l(b)}}{\chi_{s(b)}}\right)$$
$$\times\left[2\delta_{\ell 0}+\int_0^\infty dk\frac{9\Omega_{m,0}^2}{8\pi^2k^2}\left(\frac{H_0}{c}\right)^4 P_{m,0}(k)\sum_{L=2}^{\infty}(2L+1)I(\ell,L)h_L(k;\chi_{s(a)})h_L(k;\chi_{s(b)})\right]. \tag{6.21}$$

We note that we get an angular power spectrum in units of time squared, which is expected as we are computing correlators of time delays.

7 Forecasting and LSST survey

In order to obtain a realistic prediction that we can subsequently compare to measured values, we will need a reliable mock dataset of strong lenses. To this end, we consider the dataset produced by Oguri and Marshall in [27] – which seeks to mimic the upcoming LSST survey [20] by means of a semi-analytic technique based on Monte Carlo realizations of lens and source populations. In this chapter, we will describe the relevant properties of the strong lenses within the mock dataset, which are simulated in a ΛCDM universe, and the adjustments that we will have to make to apply our formalism.

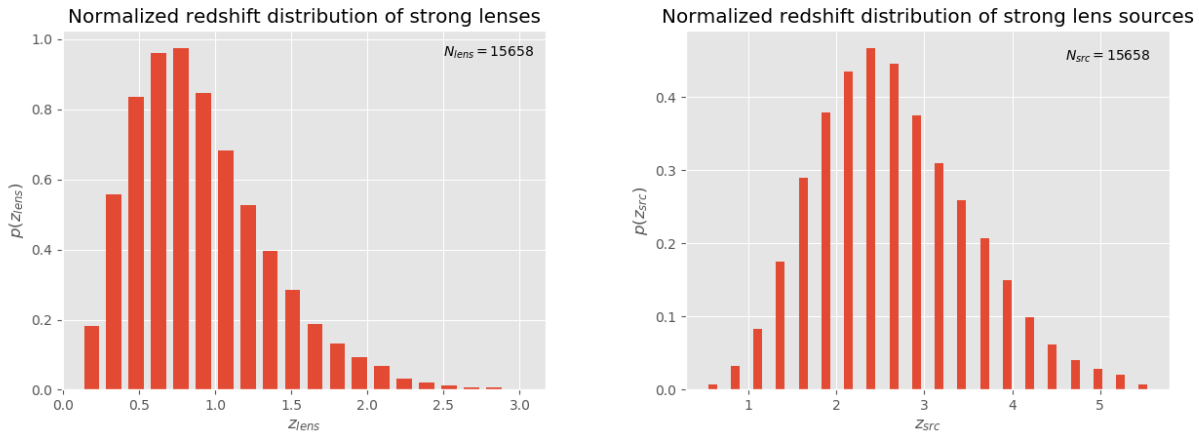

Figure 7.1: The bare probability distributions of the strong lenses and sources as a function of the redshift. Note that in both cases, $N = 15658$, as for each lens there is also a single source.

The bare data includes strong gravitational lenses that produce over 2 images. However, lenses with more than 2 images are strictly elliptical, and our formalism is limited to the case of the singular isothermal sphere. Therefore, we must filter our data to only account for 2-image lenses. In doing so, we are left with the following distributions.

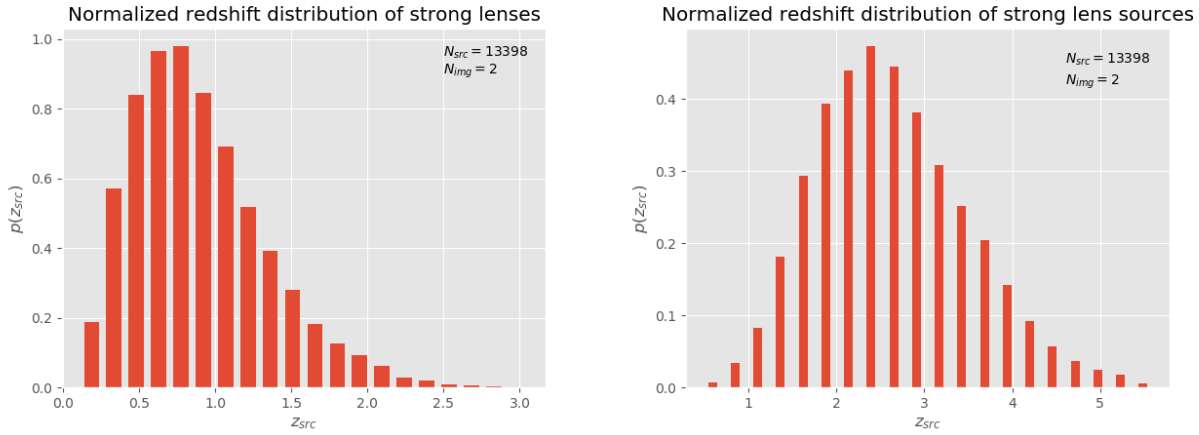

Figure 7.2: The bare probability distributions of the strong lenses and sources as a function of the redshift, now restricted to two images per lens. Note that we have discarded just over 2000 of the strong lenses.

Another factor that we must consider is the ellipticity of the lenses. As our formalism is restricted to

the spherical case, a severely top-heavy distribution here would increase inaccuracies in the final results. However, we do not want to needlessly restrict the dataset, as it should be sufficiently large.

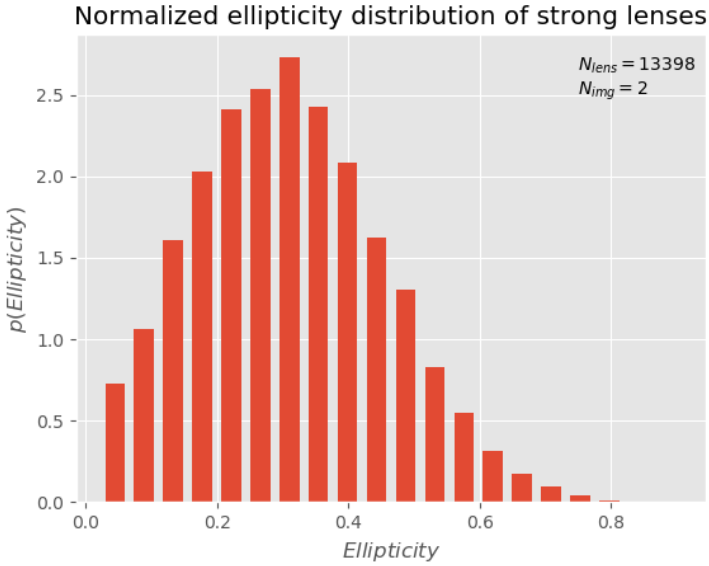

Figure 7.3: The bare probability distributions of the strong lenses as a function of the ellipticity, restricted to two images per lens. We note that the distribution is not very top-heavy, as it peaks between ellipticities of 0.2 and 0.4. To this end, we do not apply any further ellipticity filters to the dataset.

One final distribution that we will need is that of the velocity dispersion, as it enters in most of the expressions that we are interested in. We will apply all of the aforementioned filters in this plot.

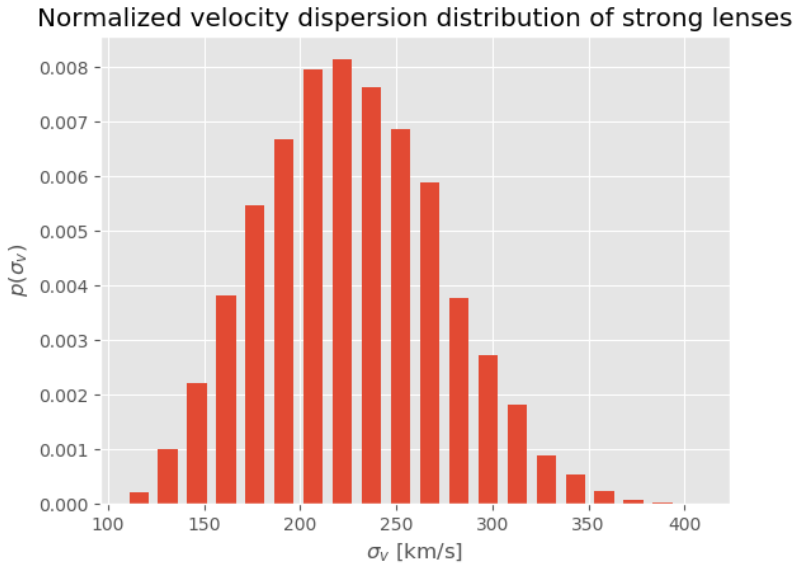

Figure 7.4: The bare probability distributions of the strong lenses as a function of the velocity dispersion.

8 Prospects for the weak lensing contaminant

In this section, we will present the results for the weak lensing contaminant derived in section 6. As mentioned, this model is considered in regular ΛCDM, and acts as a contaminant on top of the fluctuations from the dark energy model.

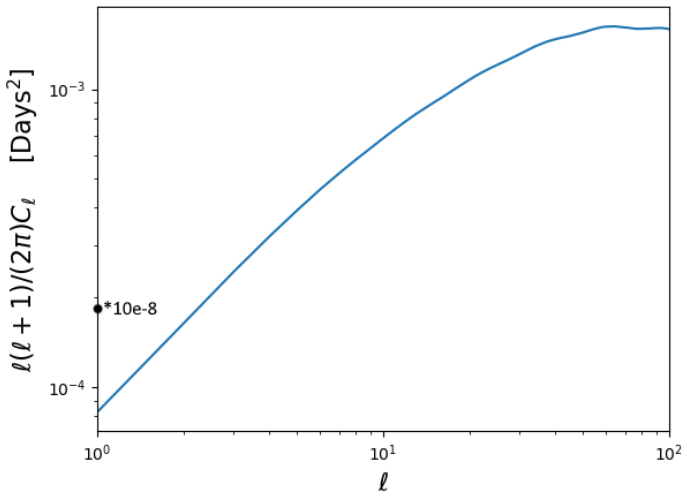

Figure 8.1: The angular power spectrum of the weak lensing contaminant in units of days squared. This has been computed in regular ΛCDM. Do note that the monopole $C_0 \approx 1.85 \cdot 10^5$ days^2 – which has been marked here explicitly as $(\bullet) \cdot 10^{-8}$ – is roughly eight orders of magnitude larger than C_ℓ when $\ell > 0$.

Observing the angular power spectrum of the weak lensing contaminant, we can assume that, despite the depth of modern surveys, correlations in the weak lensing potential due to large differences in redshift may not yet play a major part in our observations. The reason we state this is because of the large disparity between the monopole C_0 and the subsequent modes, which are roughly six orders of magnitude smaller. In order to fully understand the influence of this contaminant on the dark energy model, one would need to calculate the signal-to-noise ratio of both angular power spectra, and subsequently compare the two. We did not get to this within the timeframe of this project. However, this would be a good next step.

9 Dark energy model

In this section, we will detail the model that we intend to use in order to numerically solve the dark energy model. We previously had a purely phenomenological model. However, as we will see in this section, we can very naturally acquire a realization of this model by means of a non-minimally coupled light scalar field Φ. Note that this is not the gravitational potential Φ from before. We describe this model [17] with the action

$$S[\Phi] = \int d^4x\sqrt{-g}\left(-\frac{1}{2}g^{\mu\nu}\partial_\mu\Phi\partial_\nu\Phi - \frac{1}{2}m^2\Phi^2 - \frac{1}{2}\xi\mathcal{R}\Phi^2\right), \tag{9.1}$$

where the non-minimal coupling $-\frac{1}{2}\xi\mathcal{R}\Phi^2$ gives the field an effective mass $M^2 = m^2 + \xi\mathcal{R}$, and $\mathcal{R}$ is the Ricci scalar. In the context of an FLRW universe, this action becomes

$$S[\Phi] = \int dx\mathcal{L}_\Phi = \int dx\left[\frac{1}{2}\dot{\Phi} - \frac{1}{2a^2}(\vec{\nabla}\Phi)^2 - \frac{1}{2}(m^2 + 6\xi(2-\epsilon)H^2)\Phi^2\right]a^3, \tag{9.2}$$

where we introduced the slow roll parameter $\epsilon \equiv -\frac{\dot{H}}{H^2}$. The canonical momentum is then

$$\Pi(x) = \frac{\partial\mathcal{L}_\Phi}{\partial\dot{\Phi}(x)} = a^3\dot{\Phi}(x). \tag{9.3}$$

The corresponding Hamiltonian

$$H[\Phi;t) = \int d^3x\left\{\frac{1}{2a^3}\Pi^2 + \frac{a}{2}(\vec{\nabla}\Phi)^2 + \frac{a^3}{2}\left[m^2 + 6\xi(2-\epsilon)H^2\right]\Phi^2\right\}, \tag{9.4}$$

can be canonically quantized by promoting the field and its conjugate momenta to operators and their Poisson brackets to equal-time commutation relations:

$$\left[\hat{\Phi}(t,\vec{x}),\hat{\Pi}(t,\vec{x}')\right] = i\delta^3(\vec{x}-\vec{x}'), \qquad \left[\hat{\Phi}(t;\vec{x}),\hat{\Phi}(t,\vec{x}')\right] = 0, \qquad \left[\hat{\Pi}(t;\vec{x}),\hat{\Pi}(t,\vec{x}')\right] = 0. \tag{9.5}$$

The equations of motion for the field operators then are

$$\frac{d}{dt}\hat{\Phi}(t,\vec{x}) - a^{-3}\hat{\Pi}(t,\vec{x}) = 0, \tag{9.6}$$

$$a^{-3}\frac{d}{dt}\hat{\Pi}(t,\vec{x}) - \frac{\nabla^2}{a^2}\Phi(t,\vec{x}) + M^2(t)\hat{\Phi}(t,\vec{x}) = 0. \tag{9.7}$$

We can expand the field operators in terms of Fourier modes by means of the creation and annihilation operators $\hat{b}$ and $\hat{b}^\dagger$,

$$\hat{\Phi}(t,\vec{x}) = \int\frac{d^3k}{(2\pi)^{3/2}}\left[e^{i\vec{k}\cdot\vec{x}}\varphi(t,k)\hat{b}(\vec{k}) + \text{h.c.}\right], \tag{9.8}$$

$$\hat{\Pi}(t,\vec{x}) = \int\frac{d^3k}{(2\pi)^{3/2}}\left[e^{i\vec{k}\cdot\vec{x}}\dot{\varphi}(t,k)\hat{b}(\vec{k}) + \text{h.c.}\right]. \tag{9.9}$$

Due to spatial isotropy (which manifests as the appearance of the Laplacian operator in (9.7)), there is only a dependence on the norm of the wavevector $||\vec{k}|| = k$ in the mode function φ. The creation and annihilation operators must satisfy the typical commutation relations

$$[\hat{b}(\vec{k}),\hat{b}^\dagger(\vec{k}')] = \delta^3(\vec{k}-\vec{k}'), \qquad [\hat{b}(\vec{k}),\hat{b}(\vec{k}')] = [\hat{b}^\dagger(\vec{k}),\hat{b}^\dagger(\vec{k}')] = 0. \tag{9.10}$$

Due to this, we acquire a constraint for the mode function; the Wronskian normalization condition

$$\varphi(t,k)\dot{\varphi}^*(t,k) - \dot{\varphi}(t,k)\varphi^*(t,k) = i/a^3. \tag{9.11}$$

The equation of motion for φ inferred from (9.6) and (9.7) is then

$$\ddot{\varphi}(t,k) + 3H\dot{\varphi}(t,k) + \left[\frac{k^2}{a^2} + M^2(t)\right]\varphi(t,k) = 0. \tag{9.12}$$

The Hilbert space of states is now constructed in the typical manner. We define a vacuum state $|\Omega\rangle$ that is annihilated by the annihilation operators $\hat{b}(\vec{k})|\Omega\rangle = 0, \forall \vec{k}$. The rest of the states is constructed by the creation operators $\hat{b}^\dagger$ acting on $|\Omega\rangle$. We can now calculate the energy-momentum tensor, as per definition, $T_{\mu\nu} = \frac{-2}{\sqrt{-g}}\frac{\delta S}{\delta g^{\mu\nu}}$. In operator form, we find

$$\hat{T}_{\mu\nu} = \partial_\mu\hat{\Phi}\partial_\nu\hat{\Phi} - \frac{1}{2}g_{\mu\nu}g^{\alpha\beta}\partial_\alpha\hat{\Phi}\partial_\beta\hat{\Phi} - \frac{m^2}{2}g_{\mu\nu}\hat{\Phi}^2 + \xi[G_{\mu\nu} - \nabla_\mu\nabla_\nu + g_{\mu\nu}\Box]\hat{\Phi}^2, \tag{9.13}$$

where $\Box$ is the d'Alembertian operator. We assume that the energy-momentum tensor is sourced by an ideal fluid, implying that the energy density is given solely by the time component. We can further assume that we may neglect spatial gradients. This is the so-called stochastic formalism as detailed in [28]. We then acquire

$$\hat{\rho}_Q = -\langle\hat{T}^0{}_0\rangle \approx \frac{H^2}{2}\left\{\Delta_{\pi\pi} + 6\xi\Delta_{\phi\pi} + \left[6\xi + \left(\frac{m}{H}\right)^2\right]\Delta_{\phi\phi}\right\}, \tag{9.14}$$

where we defined

$$\Delta_{\pi\pi}(t,\vec{x}) \equiv \frac{1}{a^6(t)H^2(t)}\langle\hat{\pi}^2(t,\vec{x})\rangle, \quad \Delta_{\phi\pi}(t,\vec{x}) = \frac{1}{a^3(t)H(t)}\langle\{\hat{\phi}(t,\vec{x})\hat{\pi}(t,\vec{x})\}\rangle, \quad \Delta_{\phi\phi}(t,\vec{x}) = \langle\hat{\varphi}^2(t,\vec{x})\rangle. \tag{9.15}$$

Similarly, we find

$$\hat{p}_Q\delta^i_j = \hat{T}^i{}_j \approx \frac{H^2}{2}\left\{(1-4\xi)\Delta_{\pi\pi} + 2\xi\Delta_{\phi\pi} + \left[-2\xi(3-\varepsilon) + 24\xi^2(2-\varepsilon) - \left(\frac{m}{H}\right)^2(1-4\xi)\right]\Delta_{\phi\phi}\right\}. \tag{9.16}$$

To consider the spatial correlations exhibited by this particular dark energy model, we will need to consider the density-density correlator. We can observe that this will give rise to several four-point functions of operators $\hat{\Phi}$ and $\hat{\Pi}$. In order to do this, we will first describe the stochastic formalism introduced in [28].

9.1 Stochastic Formalism

When considering a light scalar field, the dominant contribution to the correlators in inflation will come from the superhorizon modes ($k < aH$). For very light or massless scalar fields, this is also true for the subsequent epochs of the universe, namely the matter and radiation periods. In order to formalize this, let us split the fields into long and short wavelength modes:

$$\hat{\Phi}(t,\vec{x}) = \hat{\varphi}(t,\vec{x}) + \hat{\varphi}_s(t,\vec{x}), \qquad \hat{\Pi}(t,\vec{x}) = \hat{\pi}(t,\vec{x}) + \hat{\pi}_s(t,\vec{x}). \tag{9.17}$$

Given some UV-cutoff $0 < \mu \ll 1$, these modes will be separated at the physical scale μH. In practice, we will implement this by means of a Heaviside θ-function. Additionally, we will consider these modes in Fourier space for convenience. This nets us the following long wavelength modes:

$$\hat{\varphi}(t,\vec{x}) = \int\frac{d^3k}{(2\pi)^{\frac{3}{2}}}\theta(\mu aH - \|\vec{k}\|)\left[e^{i\vec{k}\cdot\vec{x}}\varphi(t,k)\hat{b}(\vec{k}) + e^{-i\vec{k}\cdot\vec{x}}\varphi^*(t,k)\hat{b}^\dagger(\vec{k})\right], \tag{9.18}$$

$$\hat{\pi}(t,\vec{x}) = \int\frac{d^3k}{(2\pi)^{\frac{3}{2}}}\theta(\mu aH - \|\vec{k}\|)\left[e^{i\vec{k}\cdot\vec{x}}\pi(t,k)\hat{b}(\vec{k}) + e^{-i\vec{k}\cdot\vec{x}}\pi^*(t,k)\hat{b}^\dagger(\vec{k})\right], \tag{9.19}$$

and the following short wavelength modes:

$$\hat{\varphi}_s(t,\vec{x}) = \int\frac{d^3k}{(2\pi)^{\frac{3}{2}}}\theta(\|\vec{k}\| - \mu aH)\left[e^{i\vec{k}\cdot\vec{x}}\varphi(t,k)\hat{b}(\vec{k}) + e^{-i\vec{k}\cdot\vec{x}}\varphi^*(t,k)\hat{b}^\dagger(\vec{k})\right], \tag{9.20}$$

$$\hat{\pi}_s(t,\vec{x}) = \int \frac{d^3k}{(2\pi)^{\frac{3}{2}}}\theta(\|\vec{k}\| - \mu aH)\left[e^{i\vec{k}\cdot\vec{x}}\pi(t,k)\hat{b}(\vec{k}) + e^{-i\vec{k}\cdot\vec{x}}\pi^*(t,k)\hat{b}^\dagger(\vec{k})\right]. \tag{9.21}$$

We can now split (9.6) and (9.7) into long and short wavelength parts, giving us

$$\frac{d}{dt}\hat{\varphi}(t,\vec{x}) - a^{-3}\hat{\pi}(t,\vec{x}) = \hat{f}_\varphi(t,\vec{x}), \tag{9.22}$$

$$a^{-3}\frac{d}{dt}\hat{\pi}(t,\vec{x}) + M^2(t)\hat{\varphi}(t,\vec{x}) = a^{-3}\hat{f}_\pi(t,\vec{x}). \tag{9.23}$$

In these rewritten equations of motion, the sources $\hat{f}\varphi$ and $\hat{f}_\pi$ originate from the coupling between the short and long wavelength fields, and can be expressed as

$$\hat{f}_\varphi(t,\vec{x}) = \mu aH^2(1-\varepsilon)\int \frac{d^3k}{(2\pi)^{3/2}}\delta(\|\vec{k}\| - \mu aH)\left[e^{i\vec{k}\cdot\vec{x}}\varphi(t,k)\hat{b}(\vec{k}) + e^{-i\vec{k}\cdot\vec{x}}\varphi^*(t,k)\hat{b}^\dagger(\vec{k})\right], \tag{9.24}$$

$$\hat{f}_\pi(t,\vec{x}) = \mu a^4H^2(1-\varepsilon)\int \frac{d^3k}{(2\pi)^{3/2}}\delta(\|\vec{k}\| - \mu aH)\left[e^{i\vec{k}\cdot\vec{x}}\dot{\varphi}(t,k)\hat{b}(\vec{k}) + e^{-i\vec{k}\cdot\vec{x}}\dot{\varphi}^*(t,k)\hat{b}^\dagger(\vec{k})\right]. \tag{9.25}$$

We can interpret these sources to be stochastic, so we have acquired stochastic differential equations. This is the so-called stochastic formalism. We can now consider the two-point and four-point correlators of the modes.

9.2 Two-point correlators

For the following section, it is useful to express the time variable in terms of the number of e-folds N. To do this, we use that $\frac{d}{dt} = H(t)\frac{d}{dN}$. The period between t and t_0 is then defined as $N(t) = \ln(a(t))$. Rewriting (9.6) and (9.7) in terms of e-folds and the functions (9.15) nets us

$$n_{\varphi\varphi} = \frac{d}{dN}\Delta_{\varphi\varphi} - \Delta_{\varphi\pi}, \tag{9.26}$$

$$n_{\varphi\pi} = \frac{d}{dN}\Delta_{\varphi\pi} + (3-\epsilon)\Delta_{\varphi\pi} - 2\Delta_{\pi\pi} + 2\left(\frac{M}{H}\right)^2\Delta_{\varphi\varphi}, \tag{9.27}$$

$$n_{\pi\pi} = \frac{d}{dN}\Delta_{\pi\pi} + 2(3-\epsilon)\Delta_{\pi\pi} + \left(\frac{M}{H}\right)^2\Delta_{\varphi\pi}. \tag{9.28}$$

We can now re-express these in terms of the stochastic noise functions $\hat{f}$:

$$n_{\varphi\varphi} = \frac{1}{H(t)}\left\langle\left\{\hat{f}_\varphi(t,\vec{x}),\hat{\varphi}(t,\vec{x})\right\}\right\rangle, \tag{9.29}$$

$$n_{\varphi\pi} = \frac{1}{a^3(t)H^2(t)}\left[\left\langle\left\{\hat{f}_\varphi(t,\vec{x}),\hat{\pi}(t,\vec{x})\right\}\right\rangle + \left\langle\left\{\hat{f}_\pi(t,\vec{x}),\hat{\varphi}(t,\vec{x})\right\}\right\rangle\right], \tag{9.30}$$

$$n_{\pi\pi} = \frac{1}{a^6(t)H^3(t)}\left\langle\left\{\hat{f}_\pi(t,\vec{x}),\hat{\pi}(t,\vec{x})\right\}\right\rangle. \tag{9.31}$$

We want to obtain predictions for these correlators at late times. However, the formalism only nets us the original correlators. As such, we will need to evolve them through the various epochs of our universe. First inflation, then radiation domination, and then matter domination.

9.2.1 Inflation

Let us first consider the de Sitter inflationary period. To this end, we will use the Chernikov–Tagirov–Bunch –Davies (CTBD) mode function of the scalar [29], which is given by

$$\varphi(t,k) = \sqrt{\frac{\pi}{4a^3 H_I}} H^{(1)}_{\nu_I}\left(\frac{k}{aH_I}\right), \quad \nu_I = \sqrt{\frac{9}{4} - 12\xi - \left(\frac{m}{H_I}\right)^2}. \tag{9.32}$$

We can calculate the correlators n using this mode function, and plug them in to evolve the Δ through time with the corresponding equations of motion. In particular, it was shown in [17] that, given $\xi < 0$ and $(m/H_I)^2 \ll |\xi| \ll 1$, we can derive

$$\Delta_2(N_I) \equiv (\Delta_{\varphi\varphi}, \Delta_{\varphi\pi}, \Delta_{\pi\pi}) \approx \frac{H_I^2}{32\pi^2|\xi|} e^{8|\xi|N_I}\left(1, 8|\xi|, 16\xi^2\right). \tag{9.33}$$

Herein, N_I is the number of inflationary e-folds. We can now write ρ_Q and p_Q in terms of these correlators:

$$\rho_Q = -\frac{3H_I^4}{32\pi^2} e^{8|\xi|N_I}, \qquad \rho_Q = -p_Q. \tag{9.34}$$

We thus make the curious observation that, by the end of the inflationary period, our field behaves like a cosmological constant ($\rho_Q = -p_Q$). We can now continue into the radiation period by using $\Delta_2(N_I)$ as initial conditions.

9.2.2 Radiation and matter

We can approach the radiation era in a similar way, namely by using the mode functions to calculate the corresponding correlators. One key observation that allows for the somewhat straightforward time evolution of these correlators is that stochastic sources in the equations of motion can safely be neglected in post-inflationary eras, as the other terms become sufficiently enhanced in comparison. Including the radiation era, we find

$$\rho_Q = \frac{3H_I^4}{32\pi^2} e^{8|\xi|N_I}\left[-\left(\frac{H}{H_I}\right)^2 + \frac{1}{6|\xi|}\left(\frac{m}{H_I}\right)^2\right], \tag{9.35}$$

$$p_Q = \frac{3H_I^4}{32\pi^2} e^{8|\xi|N_I}\left[-\frac{1}{3}\left(\frac{H}{H_I}\right)^2 - \frac{1}{6|\xi|}\left(\frac{m}{H_I}\right)^2\right]. \tag{9.36}$$

Applying a similar reasoning as for the radiation era, we can simplify the equations for the matter era. One notable feature of the matter era is that there is an exponential contribution to the correlators, one which was discovered in the recent publication [19]. Taking this contribution into consideration, we retrieve the following correlator in the matter era:

$$\Delta_{\varphi\varphi}(N_M) = \frac{H_I^2}{32\pi^2|\xi|} e^{8|\xi|N_I + 4|\xi|N_M}, \tag{9.37}$$

where N_M is the number of e-folds after matter-radiation equality. Using $\epsilon = 3/2$, we can derive another pair of expressions for the pressure and density, now at the end of the matter era:

$$\rho_Q(N_M) \approx \frac{H^2}{2}\left[\left(\frac{m}{H}\right)^2 - 6|\xi|\right]\Delta_{\varphi\varphi}(N_M), \tag{9.38}$$

$$p_Q(N_M) \approx -\frac{m^2}{2}\Delta_{\varphi\varphi}(N_M). \tag{9.39}$$

This pair of expressions is, due to the approximations that were made, valid at leading order in $|\xi|$ and $\frac{m^2}{H^2(N_M)}$. Another notable feature is that a part of ρ_Q is found back as $-p_Q$, again displaying the cosmological

constant-like behaviour that was seen before. In addition to this, we now have an extra dark matter-like contribution in ρ_Q. If this cosmological constant term is to explain the amount of dark energy we observe today, it must abide by the following relation:

$$\frac{m^2}{2}\Delta_{\varphi\varphi}(t_0) = 3M_p^2 H_0^2 \Omega_\Lambda. \tag{9.40}$$

Using this relation, it is also possible to derive a constraint for the length of the inflationary period. Namely, it needs to be long enough to produce the amount of dark energy we observe today. We can thus find that

$$N_I = \frac{1}{8|\xi|}\ln\left[24\pi|\xi|\left(\frac{m_p}{H_I}\right)^2\left(\frac{H_{DE}}{m}\right)^2\right] - \frac{1}{2}\ln\left(\frac{\Omega_M}{\Omega_R}\right), \tag{9.41}$$

where, per definition, $\ln\left(\frac{\Omega_M}{\Omega_R}\right) = N_M(t_0)$. Furthermore, m_p is the Planck mass, $H_{DE}^2 = \Omega_\Lambda H_0^2$, and H_I is the inflationary Hubble parameter. Due to observational constraints [30], we can reasonably choose $H_I \approx 10^{13}$ GeV, which is around the GUT scale. We must also satisfy a few constraints:

$$|\xi| < \frac{1}{6}\left(\frac{m}{H_{DE}}\right)^2, \qquad \xi < 0, \qquad m/H_{DE} < 1. \tag{9.42}$$

The first constraint implies that the part of $\langle\hat{\rho}_Q\rangle$ that acts as a cosmological constant is greater than the dark matter-like contribution. The other two constraints imply a light field and a negative non-minimal coupling, which we require due to the usage of the stochastic formalism- they serve to better enhance the quantum fluctuations.

9.3 Four-point correlators

We will now take a look at the results for four-point correlators, which become relevant when the describing spatial correlations. This makes sense, as taking the two-point correlator of the density $\hat{\rho}_Q$ is what gives rise to spatial correlations. Naturally, the presence of additional terms increases the complexity of the problem, giving rise to systems of six coupled differential equations. Rather than re-deriving these values, we will simply state the results as derived in [19]. For the field correlators, we get:

$$\begin{aligned}\Delta_4(N_M, r) &\equiv \left(\Delta_{\varphi^2,\varphi^2}, \Delta_{\varphi^2,\varphi\pi}, \Delta_{\varphi\pi,\varphi\pi}, \Delta_{\varphi^2,\pi^2}, \Delta_{\varphi\pi,\pi^2}, \Delta_{\pi^2,\pi^2}\right) \\ &\approx \Delta_{\varphi\varphi}^2(N_M)s(r)\left(1, 8|\xi|, 16\xi^2, 8\xi^2, 32|\xi|^3, 16\xi^4\right).\end{aligned} \tag{9.43}$$

Herein, $r = |\chi_1 - \chi_2|$ is the comoving distance between the coordinates associated with the two components of the correlators. We also note that we get the same $\Delta_{\varphi\varphi}$ that we had in (9.37). For the spatial dependence, we acquire an s-function defined as follows:

$$s(r) \approx \begin{cases} 3, & 0 \le \mu a_{in} H_I r < e^{-N_I}, \\ 3 - 2(\mu a_{in} H_I r)^{16|\xi|}, & e^{-N_I} < \mu a_{in} H_I r < 1, \\ 1, & \mu a_{in} H_I r \ge 1. \end{cases} \tag{9.44}$$

Herein, $r_0 = (\mu a_{in} H_I)^{-1}$, which is the comoving Hubble radius at the beginning of inflation. Finally, we can write the density-density correlator – now expressed with $\vec{x} = (\chi, \chi\vec{\theta})$ – in terms of these field correlators:

$$\begin{aligned}\langle\hat{\rho}_Q(t,\vec{x})\hat{\rho}_Q(t,\vec{x}')\rangle \approx{}& \frac{H^4}{4}\left\{\left[\left(\frac{m}{H}\right)^2 + 6\xi\right]\Delta_{\varphi^2,\varphi^2} + 6\xi\left[\left(\frac{m}{H}\right)^2 + 6\xi\right]\Delta_{\varphi^2,\varphi\pi} + 36\xi^2\Delta_{\varphi\pi,\varphi\pi}\right\} \\ &+ \frac{H^4}{4}\left\{\left[\left(\frac{m}{H}\right)^2 + 6\xi\right]\Delta_{\varphi^2,\pi^2} + 6\xi\Delta_{\varphi\pi,\pi^2} + \Delta_{\pi^2,\pi^2}\right\}.\end{aligned} \tag{9.45}$$

Combining (9.38), (9.43), and (9.45) and considering the leading order in $|\xi|$ and $\frac{m^2}{H^2(N_M)}$ now gives us exactly the phenomenological result that we saw in section 3 when $\hat{\rho} \propto \hat{\varphi}^2$:

$$\langle \hat{\rho}_Q(N_M, \vec{x}) \hat{\rho}_Q(N_M, \vec{y}) \rangle \approx \langle \hat{\rho}_Q(N_M) \rangle^2 s(r). \tag{9.46}$$

This implies that we can use all of the pre-established formalism to study this particular realization of the phenomenological model as well.

9.4 Effects of a reduced speed of sound

One adjustment that we can make to this specific realization is the speed of sound c_s, which denotes the speed of the field propagations. In particular, the case we considered before assumed $c_s = 1$ so that our fields propagate at the speed of light. However, it is possible to reduce the speed of sound in this model, as was studied in [17, 19]. If we consider the speed of sound to be some constant that is not equal to the speed of light, it will enter the equation of motion for the mode function as a mere rescaling, i.e.

$$\ddot{\varphi}(t,k) + 3H\dot{\varphi}(t,k) + \left[c_s^2 \frac{k^2}{a^2} + M^2(t) \right] \varphi(t,k) = 0. \tag{9.47}$$

This rescaling carries through into all other equations that involve the wavevector k, so the mode functions become

$$\varphi(t,k) = \sqrt{\frac{\pi}{4a^3 H_I}} H^{(1)}_{\nu_I}\left(\frac{c_s k}{a H_I} \right), \quad \nu_I = \sqrt{\frac{9}{4} - 12\xi - \left(\frac{m}{H_I} \right)^2}. \tag{9.48}$$

Analogous treatment of these mode functions then leads to a rescaled field correlator, and subsequently a rescaled energy density:

$$\Delta_{\varphi\varphi}(N_M) = c_s^{-3} \frac{H_I^2}{32\pi^2|\xi|} e^{8|\xi|N_I + 4|\xi|N_M}, \tag{9.49}$$

$$\rho_Q(N_M) \approx \frac{H^2}{2} \left[\left(\frac{m}{H} \right)^2 - 6|\xi| \right] c_s^{-3} \frac{H_I^2}{32\pi^2|\xi|} e^{8|\xi|N_I + 4|\xi|N_M}. \tag{9.50}$$

Finally, the amount of e-folds required to produce enough dark energy in the inflationary period decreases due to this rescaling:

$$N_I = \frac{1}{8|\xi|} \ln \left[24\pi|\xi| \left(\frac{m_p}{H_I} \right)^2 \left(\frac{H_{DE}}{m} \right)^2 c_s^3 \right] - \frac{1}{2} \ln \left(\frac{\Omega_M}{\Omega_R} \right). \tag{9.51}$$

This final observation can be understood by noting that a reduced speed of sound leads to a longer wavelength. As quantum correlators are mostly built from long wavelength (small k) modes (part of the reason why we can employ the stochastic formalism), this acts as an enhancement for these correlators.

10 Prospects for the dark energy model

In order to compare this realization of the dark energy model to observables, we must first consider and derive values for the relevant model parameters.

10.1 Model parameters

We will consider the classical and quantum contributions to the energy density by means of the energy fractions:

$$\Omega_Q(z) = \frac{\langle\hat{\rho}_Q\rangle(z)}{3M_p^2\bar{H}^2(z)}, \qquad \Omega_c(z) = \frac{\rho_c(z)}{3M_p^2\bar{H}^2(z)}, \tag{10.1}$$

where $\Omega_Q(z) + \Omega_c(z) = 1$. We will neglect the exponential contribution from the matter era mentioned in section 9, which nets us the following redshift dependence:

$$\frac{\langle\hat{\rho}_Q\rangle(z)}{\langle\hat{\rho}_Q\rangle(0)} = \frac{\Omega_\Lambda - \frac{1}{\alpha}\frac{\bar{H}^2(z)}{H_0^2}}{\Omega_\Lambda - \frac{1}{\alpha}}. \tag{10.2}$$

Herein, we have $\Omega_\Lambda = 1 - \Omega_M$, which is the energy fraction contributed by dark energy today. We also defined the rescaled mass parameter α, implying that the constraints (9.42) have to be rewritten:

$$\alpha = \frac{1}{6|\xi|}\left(\frac{m}{H_{DE}}\right)^2, \qquad |\xi| < \frac{1}{6\alpha}, \qquad \alpha > 1, \qquad \xi < 0. \tag{10.3}$$

Writing the classical and quantum energy fractions in terms of the dressed fractions yields the following combination in our adjusted model:

$$1 = \Omega_c(z) + \Omega_Q(z) = \Omega_{0,c}(1+z)^3\frac{H_0^2}{\bar{H}^2(z)} + \left[\Omega_\Lambda\frac{H_0^2}{\bar{H}^2(z)} - \frac{1}{\alpha}\right]. \tag{10.4}$$

Note that we assumed that all classical matter scales as non-relativistic matter, hence the dependence on $(1+z)^3$. We can now rewrite the Hubble rate in terms of these energy fractions by using $\Omega_{0,c} = \Omega_M + \frac{1}{\alpha}$, yielding

$$\frac{\bar{H}^2(z)}{H_0^2} = \frac{(\Omega_M + \frac{1}{\alpha})(1+z)^3 + \Omega_\Lambda}{1 + \frac{1}{\alpha}}. \tag{10.5}$$

Note that this reduces to the regular Friedmann equation when $\alpha \to \infty$, as we will then retrieve a minimal coupling. We can conclude that

$$\Omega_Q(z) = \frac{\Omega_\Lambda - \frac{1}{\alpha}(\Omega_M + \frac{1}{\alpha})(1+z)^3}{\Omega_\Lambda + (\Omega_M + \frac{1}{\alpha})(1+z)^3}. \tag{10.6}$$

We can now consider some of the model constants. In particular, we can match this realization to our phenomenological model as described in section 3 by adopting the following values:

$$n_{DE} = 16|\xi|, \qquad r_0 = \frac{1}{\mu a_{in} H_I} \qquad s(r) = \begin{cases} 3 - 2(\mu a_{in} H_I r)^{16|\xi|}, & \mu a_{in} H_I r < 1, \\ 1, & \mu a_{in} H_I r > 1. \end{cases} \tag{10.7}$$

We thus relate our spectral slope n_DE to the non-minimal coupling ξ, and our reference scale r_0 to the energy scale at the beginning of inflation, of which a_I and H_I denote the scale factor and Hubble parameter, respectively. At the end of inflation, we will have the following Friedmann equation assuming instant reheating:

$$\frac{H_I^2}{H_0^2} = \Omega_R a_e^{-4} + \Omega_M a_e^{-3} + \Omega_\Lambda, \tag{10.8}$$

where $a_e = a_{in}e^{N_I}$ is the scale factor at the end of inflation, and $\Omega_R = 9.1 \cdot 10^{-5}$ is the energy fraction in radiation today. We can use that $a_e \ll 1$ to find

$$a_{in} = \Omega_R \left(\frac{H_I}{H_0}\right)^{-\frac{1}{2}} e^{-N_I}, \tag{10.9}$$

and subsequently the characteristic length scale

$$H_0 r_0 = \mu^{-1} e^{N_I} \left(\frac{H_I}{H_0}\right)^{-\frac{1}{2}} \Omega_R^{-\frac{1}{4}}. \tag{10.10}$$

Finally, we can combine this with (9.51) to find that

$$r_0 H_0 \approx \mu^{-1} \left(\frac{H_0\sqrt{\Omega_R}}{H_I \Omega_M}\right)^{\frac{1}{2}} \left[\frac{4\pi}{\alpha}\left(\frac{m_P}{H_I}\right)^2 c_s^3\right]^{\frac{1}{8|\xi|}}. \tag{10.11}$$

As mentioned before, $H_I \approx 10^{13}$ GeV and $\Omega_R = 9.1 \cdot 10^{-5}$. Additionally, $\Omega_M = 0.31$, $\Omega_\Lambda \approx 0.69$ and $H_0 \approx 10^{-33}$ eV. Due to the constraints (10.3), we are rather limited in which values we can select for α and ξ. A reasonable selection for these would be:

α	$\lvert\xi\rvert$
1	$[0.03, 0.065]$
2	$[0.03, 0.06]$
3	$[0.03, 0.055]$
4	$[0.028, 0.041]$
5	$[0.029, 0.033]$

We would then take $n_{DE} = 16|\xi|$ for the spectral slope. It would additionally be useful to investigate the effects of a reduced speed of sound, i.e. $c_s = 0.1$ in addition to $c_s = 1$.

11 Conclusion and discussion

11.1 Conclusion

We explored the consequences of considering a model with spatial correlations in dark energy due to fluctuations. First, we did this by means of a phenomenological model where the fluctuations stem from a quantum field. Honing in on the case where $\langle \rho_Q \rangle \propto \hat{\varphi}^2$, where $\hat{\varphi}$ is a Gaussian field, we were able to use existing results that calculate how the Hubble parameter becomes dressed by these fluctuations [17] to derive new results.

In particular, we were able to derive an expression for the dressed time delays of strong gravitational lenses, which we found differed from regular ΛCDM due to the dependence of time delays on several comoving distances. As comoving distances explicitly depend on the Hubble parameter, the fluctuations naturally carried through into the time delays.

Additionally, we explored the effects of weak gravitational lensing as a contaminant, in particular in the context of modern, deep surveys such as LSST [20]. In doing so, we found that terms of the angular power spectrum beyond the monopole contribute negligibly, implying that the WL correlator is well below the expected noise even in deeper surveys – this means it would be difficult to observe. In order to say anything about the effects of this contaminant on the fluctuating dark energy model, we would need to compare the two.

We then focused our attention on a specific realization of the aforementioned phenomenological model, exploring its parameter space, choosing potential values for the associated model constants, and exploring the idea of a reduced speed of sound.

11.2 Discussion

The logical next step for this research would be to calculate the signal-to-noise ratios (SNRs) for the various angular power spectra. In doing so, one would acquire an idea on whether this effect is observable or not, and be able to better compare the WL correlator to the DE model.

A natural follow-up to this research would be to check whether this model can alleviate tensions in cosmological parameters other than H_0. An earlier work [19] confirmed that this model can alleviate the Hubble tension, so a logical next question would be whether it can do this with the σ_8 tension too.

Another consideration could be the effect of employing this kind of model for dark matter, giving rise to dark matter with quantum fluctuations. One could then probe the effects of these fluctuations on cosmological observables such as luminosity distances and time delays, analogously to what we did here. One could extend this idea further by coupling dark matter and dark energy.

Additionally, with our eyes on upcoming gravitational wave experiments, it would be interesting to study the effects of this kind of model on gravitational wave formalism.

Finally, one could extend the formalism introduced here to other probes such as the cosmic microwave background.

Acknowledgements

As we have come to the conclusion of this work, I would like to express my heartfelt appreciation to the individuals whose support was instrumental in allowing me to complete this work.

First, I would like to thank my daily supervisor Enis Belgacem for so graciously letting me come over to his office and arranging so many meetings in order to guide me whenever I got stuck (which, admittedly, was quite often). You have been a great teacher throughout this entire process, my sincerest thanks.

Next, I would like to thank my first supervisor Elisa Chisari, who always supported the process by means of her great knowledge of observational cosmology, and further supported me with some of the finer details when it came to the numerical methodology, which turned out to be tougher than expected in this project. I really appreciate the extra time she took to help me out with these issues, despite her already busy schedule. On a sidenote, I also appreciate some of the more personal conversations we were able to have.

Naturally, I would also like to thank my second supervisor Tomislav Prokopec, who was every bit as involved in the project, and offered great theoretical knowledge and interesting perspectives that often helped with the theoretical conundrums that we stumbled upon. Although I regularly fail to completely understand some of your more theoretical explanations, they remain one of my favourite parts of the entire degree.

Additionally, I would also like to extend my thanks to the Large Scale Structure group, whose weekly discussions gave me a proper taste of what scientific collaboration feels like, and helped me learn more about modern cosmology in general.

On a more personal note, I would like to thank some of my peers in Giovanni, Audrique, Mithuss, Prajit, Alek, George, and Liam, as their presence and support regularly motivated me. There's no support like having peers working towards the same goal surrounding you. I would also like to thank both Rin and Sophie for being a stable presence and providing moral support.

Last but not least, thanks Eden. Your constant reassurance and unwavering faith in me pushed me forward when the process got particularly tough.

A Derivation of the luminosity distance

The observed flux F at a distance d from a source of luminosity L is given by

$$F = \frac{L}{4\pi d^2}, \tag{A.1}$$

which is simply the luminosity dispersed over the area of a sphere of radius d. We can generalize this expression to an expanding universe by adapting our definition of the luminosity to a comoving spherical shell, and further replacing the regular distance by a comoving distance to get

$$F = \frac{L(a)}{4\pi\chi^2(a)}. \tag{A.2}$$

We can note that $L(\chi)$ will be twice-affected by the expanding universe. Once by the comoving grid, which will impose smaller physical distances for the photons at early times as opposed to late times, making the amount of photons crossing a shell in a fixed time interval smaller by a factor a- and once by redshifting the energy of the photons by a factor a, giving us

$$F = \frac{La^2}{4\pi\chi^2(a)}. \tag{A.3}$$

We therefore define the luminosity distance

$$d_L(a) \equiv \frac{\chi}{a} \tag{A.4}$$

so that we can express (A.1) in the comoving sphere by simply replacing d with d_L.

B Vanishing components of the singular isothermal sphere

When considering the time delays for the singular isothermal sphere, we stumble upon components that are linear in Θ that are divergent. However, said divergences cancel each other out as follows:

$$\Theta^{(a)} - \Theta^{(b)} = \frac{1}{c^2}\int_{-\infty}^{\infty} ds(\Phi_a - \Phi_b)$$

$$= \frac{2\sigma_v^2}{c^3}\int_{-\infty}^{\infty} \ln\left(\sqrt{\frac{r_{\perp,a}^2 + s^2}{r_{\perp,b}^2 + s^2}}\right)$$

$$= \frac{2\sigma_v^2}{c^3}\left[\frac{s}{2}\ln\left(\frac{r_{\perp,a}^2 + s^2}{r_{\perp,b}^2 + s^2}\right) + r_{\perp,a}\arctan\left(\frac{s}{r_{\perp,a}}\right) + r_{\perp,b}\arctan\left(\frac{s}{r_{\perp,b}}\right)\right]_{-\infty}^{\infty}$$

$$= \frac{2\pi\sigma_v^2}{c^3}(r_{\perp,a} - r_{\perp,b}).$$

As for the components quadratic in Θ, they turn out to be a constant, and thus cancel each other out entirely as follows:

$$(\vec{\nabla}_\perp\Theta)^2 = \left[\frac{2\sigma_v^2}{c^3}\int_{-\infty}^{\infty} ds(\hat{e}_x\partial_x + \hat{e}_y\partial_y)\ln\left(\frac{\sqrt{x^2+y^2+s^2}}{r_0}\right)\right]^2$$

$$= \left[\frac{2\sigma_v^2}{c^3}\int_{-\infty}^{\infty} ds\frac{x\hat{e}_x + y\hat{e}_y}{x^2+y^2+s^2}\right]^2$$

$$= \left[\frac{2\pi\sigma_v^2}{c^3}\frac{x\hat{e}_x + y\hat{e}_y}{\sqrt{x^2+y^2}}\right]^2$$

$$= (\frac{2\pi\sigma_v^2}{c^3})^2\frac{x^2+y^2}{x^2+y^2}$$

$$= \frac{4\pi^2\sigma_v^4}{c^6}.$$

Therefore,

$$(\vec{\nabla}_\perp\Theta_a)^2 - (\vec{\nabla}_\perp\Theta_b)^2 = 0.$$

C Unequal time correlator

When calculating the angular power spectrum of our dark energy model, we acquire correlators of time delays at various redshifts. Given the depth of modern surveys, these redshifts can reach high values. Therefore, it is important to consider the effects of these unequal times on the correlator. To derive this correlator, we consider an expansion around today

$$\langle\hat{\rho}_Q(t_1,\hat{n}_1)\hat{\rho}_Q(t_2,\hat{n}_2)\rangle \approx \langle\hat{\rho}_Q(t_0,\hat{n}_1)\hat{\rho}_Q(t_0,\hat{n}_2)\rangle + \Delta t_1\langle\dot{\hat{\rho}}_Q(t_0,\hat{n}_1)\hat{\rho}_Q(t_0,\hat{n}_2)\rangle + \Delta t_2\langle\hat{\rho}_Q(t_0,\hat{n}_1)\dot{\hat{\rho}}_Q(t_0,\hat{n}_2)\rangle. \tag{C.1}$$

Here, we defined $\Delta t = t - t_0$, where t is the cosmological time and t_0 denotes the cosmological time today. Equivalently, t_0 denotes the age of the universe. We can now define an ansatz

$$\langle\hat{\rho}_Q(t,\hat{n}_1)\dot{\hat{\rho}}_Q(t,\hat{n}_2)\rangle = \langle\dot{\hat{\rho}}_Q(t,\hat{n}_1)\hat{\rho}_Q(t,\hat{n}_2)\rangle = B(t)\langle\hat{\rho}_Q(t)\rangle\langle\hat{\rho}_Q(t)\rangle s(\|\vec{x}-\vec{y}\|) \tag{C.2}$$

for the unequal time correlator. We can use the Leibniz rule to now derive the following:

$$\partial_t\langle\hat{\rho}_Q(t,\hat{n}_1)\hat{\rho}_Q(t,\hat{n}_2)\rangle = 2B(t)\langle\hat{\rho}_Q(t)\rangle\langle\hat{\rho}_Q(t)\rangle s(\|\vec{x}-\vec{y}\|). \tag{C.3}$$

We can additionally acquire another expression for this derivative by simply inserting the equal time correlator as defined in (3.1) into the left-hand side of (C.3):

$$\partial_t\langle\hat{\rho}_Q(t,\hat{n}_1)\hat{\rho}_Q(t,\hat{n}_2)\rangle = \left(2\frac{\langle\dot{\hat{\rho}}_Q\rangle(t)}{\langle\hat{\rho}_Q\rangle(t)}\right)\langle\hat{\rho}_Q\rangle(t)^2 s(\|\vec{x}-\vec{y}\|). \tag{C.4}$$

We can now obtain $B(t)$ by comparing (C.3) to (C.4). This gives us

$$B(t) = \frac{\langle\dot{\hat{\rho}}_Q\rangle(t)}{\langle\hat{\rho}_Q\rangle(t)}. \tag{C.5}$$

Inserting this into our original expansion, we find that

$$\langle\hat{\rho}_Q(t_1,\hat{n}_1)\hat{\rho}_Q(t_2,\hat{n}_2)\rangle \approx \langle\hat{\rho}_Q(t_0,\hat{n}_1)\hat{\rho}_Q(t_0,\hat{n}_2)\rangle\left(1 + (\Delta t_1 + \Delta t_2)\frac{\langle\dot{\hat{\rho}}_Q\rangle(t_0)}{\langle\hat{\rho}_Q\rangle(t_0)}\right). \tag{C.6}$$

It will be beneficial to write this in terms of the redshift. We can do this by noting that, at linear order, $t_0 - t \approx -H_0 z$. Therefore,

$$\langle\hat{\rho}_Q(t_1,\hat{n}_1)\hat{\rho}_Q(t_2,\hat{n}_2)\rangle \approx \langle\hat{\rho}_Q(t_0,\hat{n}_1)\hat{\rho}_Q(t_0,\hat{n}_2)\rangle\left(1 + (z_1 + z_2)\frac{\langle\hat{\rho}'_Q\rangle(z=0)}{\langle\hat{\rho}_Q\rangle(z=0)}\right). \tag{C.7}$$

D Unequal time power spectrum of the weak lensing contaminant

In the calculation of the weak lensing contaminant, one acquires a time-dependent power spectrum of which the form is non-trivial. Ideally, one would expand it in a way where the resulting expressions become analytically solvable. There are several approaches that one can take when expanding this power spectrum, all of which involve the linearization of the underlying potentials with linear growth functions. In doing so, one acquires

$$\Phi(z;\vec{x}) = D_\Phi(z)\Phi(z=0;\vec{x}),$$

at which point it is trivial to expand the growth function up to linear order in redshift. Doing this with the correlator gives

$$\begin{aligned}\langle\tilde{\Phi}(z;\vec{k}')\tilde{\Phi}^*(z';\vec{k}'')\rangle &= D_\Phi(z)D_\Phi(z')\langle\tilde{\Phi}(z=0;\vec{k}')\tilde{\Phi}^*(z=0;\vec{k}'')\rangle \\ &= D_\Phi(z)D_\Phi(z')(2\pi)^3\delta^{(3)}(\vec{k}'-\vec{k}'')P_\Phi(k').\end{aligned}$$

This is to say that

$$P_\Phi(z,z',k) \approx D(z)D(z')P_\Phi(k) := P_1(z,z',k)$$

We can now expand this around today ($z=0$) as follows:

$$\begin{aligned}D_\Phi(z)D_\Phi(z')(2\pi)^3\delta^{(3)}(\vec{k}'-\vec{k}'')P_\Phi(k') &= [1+zD'_\Phi(z=0)][1+z'D'_\Phi(z=0)](2\pi)^3\delta^{(3)}(\vec{k}'-\vec{k}'')P_\Phi(k') \\ &= [1+(z+z')D'_\Phi(z=0)+zz'(D'_\Phi(z=0))^2](2\pi)^3\delta^{(3)}(\vec{k}'-\vec{k}'')P_\Phi(k').\end{aligned}$$

We can thus draw the conclusion that, when linearized with growth functions and expanded around today,

$$P_\Phi(z,z',k) \approx [1+(z+z')D'_\Phi(z=0)+zz'(D'_\Phi(z=0))^2]P_\Phi(k) := P_2(z,z',k).$$

It is also possible to expand the growth functions around some intermediate redshift $\bar{z} = \frac{z+z'}{2}$ by defining $\Delta z = |z-z'|$, which gives

$$P_\Phi(\bar{z}+\Delta z/2, \bar{z}-\Delta z/2, k) \approx \left[1-\frac{\Delta z^2}{4}\left(\frac{D'(\bar{z})}{D(\bar{z})}\right)\right]P_\Phi(\bar{z},k) := P_3(z,z',k).$$

Of these three approximations, P_2 is by far more preferable at first glance due to it leading to an expression that one can integrate analytically in χ. However, in comparing these approximations to a significantly more accurate Zeldovich approximation P^{Zel} as described in [31], we find the following ratio plots:

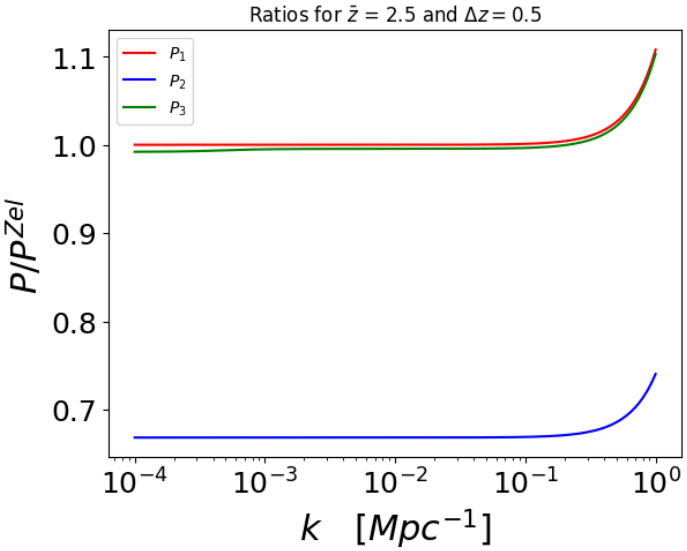

We can clearly see that P_2 – expanding around today – introduces significant errors in the final result. On the other hand, P_1 and P_3 – not expanding the potential growth functions and expanding around an intermediate redshift, respectively – are comparable in their accuracy. We are therefore led to the conclusion that we cannot approximate the power spectra to make the χ-integrals analytic in a way that does not introduce a significant source of error, which is why we opt for a numerical approach with P_1 instead.

E Derivation of the weak lensing contaminant

We start by considering a linear combination of the SL and WL potentials, i.e. the deflection angle becomes

$$\vec{\alpha} = \vec{\theta} - \vec{\beta} = \vec{\nabla}_\theta(\psi_{SL} + \psi_{WL}).$$

Writing this out in components and expanding the weak lensing contribution, we find that

$$\theta_i - \beta_i \approx \partial_i \psi_{SL}(\vec{\theta}) + \partial_i \psi_{WL}|_{\vec{\beta}} + \partial_i \partial_j \psi_{WL}|_{\vec{\beta}}(\theta_j - \beta_j)$$

$$\implies (\delta_{ij} - \partial_i \partial_j \psi_{WL}|_{\vec{\beta}})(\theta_j - \beta_j) \approx \partial_i \psi_{SL}(\vec{\theta}) + \partial_i \psi_{WL}|_{\vec{\beta}}. \tag{E.1}$$

Notably, in the singular isothermal sphere,

$$\vec{\nabla}_\theta \psi_{SL}(\vec{\theta}) = \theta_E \frac{\vec{\theta}}{||\vec{\theta}||} \implies \psi_{SL}(\vec{\theta}) = \theta_E ||\vec{\theta}|| + C$$

where $\theta_E \equiv \frac{D_{ls}}{D_s} \frac{4\pi\sigma_v^2}{c^2}$. Then, we introduce the coordinate change $\vec{x} := \frac{\vec{\theta}}{\theta_E}, \vec{y} := \frac{\vec{\beta}}{\theta_E}$, turning (1) into

$$(\delta_{ij} - \partial_i \partial_j \psi_{WL}|_{\vec{\beta}})(x_j - y_j) \approx \frac{x_i}{||\vec{x}||} + \frac{\partial_i \psi_{WL}|_{\vec{\beta}}}{\theta_E}. \tag{E.2}$$

We now want to solve for $\vec{x}$. In order to do this, let us approach the problem perturbatively, i.e. $x_i \approx x_i^{(SL)} + x_i^{(WL)}$. Then,

$$||\vec{x}||^2 = (x_i^{(SL)} + x_i^{(WL)})^2 = ||\vec{x}^{(SL)}||^2 + 2\vec{x}^{(WL)} \cdot \vec{x}^{(SL)} + \mathcal{O}((\vec{x}^{(WL)})^2)$$

$$\approx ||\vec{x}^{(SL)}||^2 \left(1 + 2\frac{\vec{x}^{(WL)} \cdot \vec{x}^{(SL)}}{||\vec{x}^{(SL)}||^2}\right),$$

and

$$\frac{1}{||\vec{x}||} \approx \frac{1}{||\vec{x}^{(SL)}||} \left(1 - \frac{\vec{x}^{(WL)} \cdot \vec{x}^{(SL)}}{||\vec{x}^{(SL)}||^2}\right).$$

Therefore, we can express the RHS as

$$\frac{x_i}{||\vec{x}||} \approx \frac{1}{||\vec{x}^{(SL)}||} \left(x_i^{(SL)} + x_i^{(WL)} - \frac{\vec{x}^{(WL)} \cdot \vec{x}^{(SL)}}{||\vec{x}^{(SL)}||^2} x_i^{(SL)}\right).$$

Now for the LHS. Writing out the brackets, we find that our starting expression will be

$$(\delta_{ij} - \partial_i \partial_j \psi_{WL}|_{\vec{\beta}})(x_j^{(SL)} + x_j^{(WL)} - y_j)$$

$$\approx x_i^{(SL)} + x_i^{(WL)} - \partial_i \partial_j \psi_{WL}|_{\vec{\beta}}(x_j^{(SL)} - y_j) - y_i.$$

Writing everything out, we need to solve the following equation for x_i:

$$x_i^{(SL)} + x_i^{(WL)} - \partial_i \partial_j \psi_{WL}|_{\vec{\beta}}(x_j^{(SL)} - y_j) - y_i$$

$$= \frac{1}{||\vec{x}^{(SL)}||} \left(x_i^{(SL)} + x_i^{(WL)} - \frac{\vec{x}^{(WL)} \cdot \vec{x}^{(SL)}}{||\vec{x}^{(SL)}||^2} x_i^{(SL)}\right) + \frac{\partial_i \psi_{WL}|_{\vec{\beta}}}{\theta_E}. \tag{E.3}$$

We will split this up in two parts. One where we take all terms that have no weak lensing, and one where we take all terms that do have weak lensing. Then, we find that

$$\mathcal{O}(\psi_{WL}^0) : x_i^{(SL)} - y_i \approx \frac{x_i^{(SL)}}{||\vec{x}^{(SL)}||} \implies \vec{x}^{(SL)} \left(1 - \frac{1}{||\vec{x}^{(SL)}||}\right) = \vec{y}.$$

This is the strong lensing solution that we already knew of. For $\vec{y} = \vec{0}$ (Source directly behind the center of the lens, i.e. intercepting the line of sight) we find an Einstein ring at $||\vec{\theta}|| = \theta_E$. When $\vec{y} \neq \vec{0}$, we note that $\vec{x}^{SL} = \alpha\vec{y}$, i.e. the source and the images are in the same direction with respect to the center of the lens. We can now discern two cases:

$$\alpha = \begin{cases} 1 + \frac{1}{||\vec{y}||} & \alpha > 0 \\ 1 - \frac{1}{||\vec{y}||} & \alpha < 0 \quad (||\vec{\beta}|| < \theta_E). \end{cases}$$

We thus conclude that we are interested in the cases where the source is within the Einstein radius ($||\vec{\beta}|| < \theta_E$), as this gives us the two images that we are interested in at

$$\vec{x}_{\pm}^{(SL)} \approx \vec{y}\left(1 \pm \frac{1}{||\vec{y}||}\right) \Longrightarrow \theta_E \vec{\theta}^{(SL)} \approx \vec{\beta} \pm \theta_E \frac{\vec{\beta}}{||\vec{\beta}||}. \tag{E.4}$$

We can now consider the weak lensing terms in (3). This gives us the following:

$$\mathcal{O}(\psi_{WL}) : x_i^{(WL)} - \partial_i\partial_j\psi_{WL}|_{\vec{\beta}}(x_j^{(SL)} - y_j) \approx \frac{1}{||\vec{x}^{(SL)}||}\left(x_i^{(WL)} - \frac{\vec{x}^{(WL)} \cdot \vec{x}^{(SL)}}{||\vec{x}^{(SL)}||^2} x_i^{(SL)}\right) + \frac{\partial_i\psi_{WL}|_{\vec{\beta}}}{\theta_E}.$$

Using our previously derived expression for $\vec{x}_{\pm}^{(SL)}$, we can find that $||\vec{x}_{\pm}^{(SL)}|| = 1 \pm ||\vec{y}||$, and our expression becomes

$$x_i^{(WL)} \mp \partial_i\partial_j\psi_{WL}|_{\vec{\beta}} \frac{y_j}{||\vec{y}||} \approx \frac{x_i^{(WL)}}{1 \pm ||\vec{y}||} - y_i \vec{x}^{(WL)} \cdot \vec{y} \frac{1 \pm \frac{1}{||\vec{y}||}}{(1 \pm ||\vec{y}||)^3} + \frac{\partial_i\psi_{WL}|_{\vec{\beta}}}{\theta_E}$$

$$\Longrightarrow x_i^{(WL)} \mp \partial_i\partial_j\psi_{WL}|_{\vec{\beta}} \frac{y_j}{||\vec{y}||} \approx \frac{x_i^{(WL)}}{1 \pm ||\vec{y}||} - \frac{y_i}{||\vec{y}||^2} \frac{x_i^{(WL)} \cdot \vec{y}}{1 \pm ||\vec{y}||} + \frac{\partial_i\psi_{WL}|_{\vec{\beta}}}{\theta_E}.$$

Isolating the terms $\vec{x}^{(WL)}$ and $\psi_{WL}|_{\vec{\beta}}$ on opposite sides, and additionally writing the dot products out component-wise brings us to the equation that we must solve:

$$x_i^{(WL)}\left(1 - \frac{1}{1 \pm ||\vec{y}||}\right) + \frac{y_i y_j x_j^{(WL)}}{(1 \pm ||\vec{y}||)||\vec{y}||^2} \approx \frac{\partial_i\psi_{WL}|_{\vec{\beta}}}{\theta_E} \pm \partial_i\partial_j\psi_{WL}|_{\vec{\beta}} \frac{y_j}{||\vec{y}||}.$$

We can now group all terms $x_j^{(WL)}$ to find that

$$\left(\frac{\delta_{ij} \pm \frac{y_i y_j}{||\vec{y}||^2}}{1 \pm \frac{1}{||\vec{y}||}}\right) x_j^{(WL)} \approx \frac{\partial_i\psi_{WL}|_{\vec{\beta}}}{\theta_E} \pm \partial_i\partial_j\psi_{WL}|_{\vec{\beta}} \frac{y_j}{||\vec{y}||}.$$

Note that this is essentially just a matrix problem, i.e.

$$M_{ij}^{\pm} x_j^{(WL)} \approx V_i^{\pm},$$

where

$$\left(1 \pm \frac{1}{||\vec{y}||}\right) M^{\pm} = \begin{pmatrix} 1 \pm \frac{y_1^2}{||\vec{y}||^3} & \pm \frac{y_1 y_2}{||\vec{y}||^3} \\ \pm \frac{y_1 y_2}{||\vec{y}||^3} & 1 \pm \frac{y_2^2}{||\vec{y}||^3} \end{pmatrix} \Longrightarrow \det M^{\pm} = \left(1 \pm \frac{1}{||\vec{y}||}\right)^{-1},$$

such that

$$(M^{\pm})_{ij}^{-1} = \left(1 \pm \frac{1}{||\vec{y}||}\right)\delta_{ij} \mp \frac{y_i y_j}{||\vec{y}||^3}.$$

We can now solve for $\vec{x}^{(WL)}$, as $x_i^{(WL)} \approx (M^{\pm})_{ij}^{-1} V_j^{\pm}$, which gives us

$$x_i^{(WL)} = \left[\left(1 \pm \frac{1}{||\vec{y}||}\right)\delta_{ij} \mp \frac{y_i y_j}{||\vec{y}||^3}\right]\left(\frac{\partial_j\psi_{WL}|_{\vec{\beta}}}{\theta_E} \pm \partial_j\partial_k\psi_{WL}|_{\vec{\beta}} \frac{y_k}{||\vec{y}||}\right).$$

$$= \left(1 \pm \frac{1}{||\vec{y}||}\right) \frac{\partial_i \psi_{WL}|_{\vec{\beta}}}{\theta_E} \pm \left(1 \pm \frac{1}{||\vec{y}||}\right) \partial_i \partial_k \psi_{WL}|_{\vec{\beta}} \frac{y_k}{||\vec{y}||} \mp \frac{y_i y_j}{||\vec{y}||^3} \frac{\partial_j \psi_{WL}|_{\vec{\beta}}}{\theta_E} - \frac{y_i y_j y_k}{||\vec{y}||^4} \partial_j \partial_k \psi_{WL}|_{\vec{\beta}}.$$

In order to simplify these expressions, we will define the normal vector $\hat{n} = \frac{\vec{\beta}}{||\vec{\beta}||}$, at which point we can rewrite terms $n_i \partial_i$ as $\partial_{\hat{n}}$. In doing so, our expression becomes

$$\vec{\theta}^{(WL)} \approx \left(1 \pm \frac{\theta_E}{||\vec{\beta}||}\right) \vec{\nabla}_{\hat{n}} \psi_{WL}|_{\vec{\beta}} \mp \frac{\theta_E}{||\vec{\beta}||} \partial_{\hat{n}} \psi_{WL}|_{\vec{\beta}} \hat{n} + \theta_E \left(\frac{\theta_E}{||\vec{\beta}||} \pm 1\right) \vec{\nabla} \partial_{\hat{n}} \psi_{WL}|_{\vec{\beta}} - \frac{\theta_E^2}{||\vec{\beta}||} \partial_{\hat{n}}^2 \psi_{WL}|_{\vec{\beta}} \hat{n}. \quad \text{(E.5)}$$

Now that we have all of the needed expressions, i.e. $\vec{\theta}^{\pm} \approx (4) + (5)$, let us go to our time delay (and neglect all terms $\mathcal{O}(\psi_{WL}^2)$):

$$t(\vec{\theta}, \vec{\beta}) = \frac{1 + z_l}{c} \frac{D_l D_s}{D_{ls}} \left[\frac{1}{2} (\vec{\nabla}_\theta \psi)^2 - \psi(\vec{\theta})\right]$$

$$\approx \frac{1 + z_l}{c} \frac{D_l D_s}{D_{ls}} \left[\frac{1}{2} ||\vec{\nabla} \psi_{SL}||^2 + \vec{\nabla} \psi_{SL} \cdot \vec{\nabla} \psi_{WL} - \psi(\vec{\theta})\right].$$

Calculating the difference between two images, we find

$$\Delta t(\vec{\theta}^{\pm}, \vec{\beta}) \approx \frac{1 + z_l}{c} \frac{D_l D_s}{D_{ls}} \Bigg\{ \frac{1}{2} ||\vec{\nabla} \psi_{SL}^+||^2 - \frac{1}{2} ||\vec{\nabla} \psi_{SL}^-||^2 + \partial_i \psi_{SL}^+ \left[\partial_i \psi_{WL}|_{\vec{\beta}} + \partial_i \partial_j \psi_{WL}|_{\vec{\beta}} (\theta_{+,j} - \beta_j)\right]$$

$$\times \partial_i \psi_{SL}^- \left[\partial_i \psi_{WL}|_{\vec{\beta}} + \partial_i \partial_j \psi_{WL}|_{\vec{\beta}} (\theta_{-,j} - \beta_j)\right] - \psi_{SL}^+ + \psi_{SL}^- - \psi_{WL}^+ + \psi_{WL}^- \Bigg\}.$$

However, we can simplify this by noting that

$$\psi(\vec{\theta}^{\pm}) = \psi_{SL}(\vec{\theta}^{\pm}) + \psi_{WL}(\vec{\theta}^{\pm}) \approx \psi_{SL}(\vec{\theta}^{\pm}) + \psi_{WL}|_{\vec{\beta}} + \partial_i \psi_{WL}|_{\vec{\beta}} (\theta_i^{\pm} - \beta_i)$$

$$\implies -\psi_{SL}^+ + \psi_{SL}^- - \psi_{WL}^+ + \psi_{WL}^- \approx -\psi_{SL}^+ + \psi_{SL}^- - \partial_i \psi_{WL}|_{\vec{\beta}} (\theta_{+,i} - \theta_{-,i}).$$

Additionally, we know that $\psi_{SL}(\vec{\theta}^{\pm}) = \theta_E ||\vec{\theta}^{\pm}|| + C$, which we can insert. Finally, we have previously calculated that (for SIS)

$$\frac{1}{2} (||\vec{\nabla} \psi_{SL}^+||^2 - ||\vec{\nabla} \psi_{SL}^-||^2) = 0.$$

Using all of this, we find that

$$\Delta t(\vec{\theta}^{\pm}, \vec{\beta}) = \frac{1 + z_l}{c} \frac{D_l D_s}{D_{ls}} \Bigg\{ \theta_E \partial_i \psi_{WL}|_{\vec{\beta}} \left(\frac{\theta_i^+}{||\vec{\theta}^+||} - \frac{\theta_i^-}{||\vec{\theta}^-||}\right) + \theta_E \partial_i \partial_j \psi_{WL}|_{\vec{\beta}} \left(\frac{\theta_i^+ \theta_j^+}{||\vec{\theta}^+||} - \frac{\theta_i^- \theta_j^-}{||\vec{\theta}^-||}\right)$$

$$-\theta_E \partial_i \partial_j \psi_{WL}|_{\vec{\beta}} \beta_j \left(\frac{\theta_i^+}{||\vec{\theta}^+||} - \frac{\theta_i^-}{||\vec{\theta}^-||}\right) - \theta_E (||\vec{\theta}^+|| - ||\vec{\theta}^-||) - \partial_i \psi_{WL}|_{\vec{\beta}} (\theta_i^+ - \theta_i^-) \Bigg\}.$$

We will now need to explicitly find an expression for the norm. Let us start from the norm squared (again, neglecting all terms $\mathcal{O}(\psi_{WL}^2)$):

$$||\vec{\theta}^{\pm}||^2 \approx \left(||\vec{\beta}|| \pm \theta_E \mp \frac{\theta_E}{||\vec{\beta}||} \partial_{\hat{n}} \psi_{WL}|_{\vec{\beta}} - \frac{\theta_E^2}{||\vec{\beta}||} \partial_{\hat{n}}^2 \psi_{WL}|_{\vec{\beta}}\right)^2$$

$$+2\partial_{\hat{n}} \psi_{WL}|_{\vec{\beta}} \left(1 \pm \frac{\theta_E}{||\vec{\beta}||}\right) (||\vec{\beta}|| \pm \theta_E) + 2\partial_{\hat{n}}^2 \psi_{WL}|_{\vec{\beta}} \theta_E \left(\frac{\theta_E}{||\vec{\beta}||} \pm 1\right) (||\vec{\beta}|| \pm \theta_E).$$

When we work out the brackets, we find that a lot of these terms cancel against each other. In fact, the remaining terms are

$$||\vec{\theta}^{\pm}||^2 \approx (||\vec{\beta}|| \pm \theta_E)^2 + 2(||\vec{\beta}|| \pm \theta_E)\partial_{\hat{n}}\psi_{WL}|_{\vec{\beta}} \pm 2\theta_E(||\vec{\beta}|| \pm \theta_E)\partial^2_{\hat{n}}\psi_{WL}|_{\vec{\beta}}$$

$$= (||\vec{\beta}|| \pm \theta_E)^2(1 + 2(||\vec{\beta}|| \pm \theta_E)^{-1}\partial_{\hat{n}}\psi_{WL}|_{\vec{\beta}} \pm 2\theta_E(||\vec{\beta}|| \pm \theta_E)^{-1}\partial^2_{\hat{n}}\psi_{WL}|_{\vec{\beta}}).$$

Note that we can then use the approximation $\sqrt{1+x} \approx 1 + \frac{x}{2}$ considering x is small. Therefore,

$$||\vec{\theta}^{\pm}|| \approx (||\vec{\beta}|| \pm \theta_E)(1 + (||\vec{\beta}|| \pm \theta_E)^{-1}\partial_{\hat{n}}\psi_{WL}|_{\vec{\beta}} \pm \theta_E(||\vec{\beta}|| \pm \theta_E)^{-1}\partial^2_{\hat{n}}\psi_{WL}|_{\vec{\beta}})$$

$$= \theta_E \pm ||\vec{\beta}|| \pm \partial_{\hat{n}}\psi_{WL}|_{\vec{\beta}} + 2\theta_E\partial^2_{\hat{n}}\psi_{WL}|_{\vec{\beta}},$$

and

$$||\vec{\theta}^{+}|| - ||\vec{\theta}^{-}|| = 2(||\vec{\beta}|| + \partial_{\hat{n}}\psi_{WL}|_{\vec{\beta}}).$$

We can now make a few observations to simplify our lives- Namely, whether we are considering $\vec{\theta}^{+}_{SL}$ or $\vec{\theta}^{-}_{SL}$ has an effect on the sign of our vector, which is to say that we have

$$\vec{\theta}^{\pm}_{SL} = \begin{cases} (||\vec{\beta}|| + \theta_E)\hat{n} & \theta^+ \\ -(\theta_E - ||\vec{\beta}||)\hat{n} & \theta^-, \end{cases}$$

and subsequently that we can argue that

$$\frac{\theta^+_i}{||\vec{\theta}^+||} \approx n_i, \quad \frac{\theta^-_i}{||\vec{\theta}^-||} \approx -n_i, \quad \frac{\theta^+_i}{||\vec{\theta}^+||} - \frac{\theta^-_i}{||\vec{\theta}^-||} \approx 2n_i.$$

Using the same reasoning, we can also argue that

$$\frac{\theta^+_i\theta^+_j}{||\vec{\theta}^+||} - \frac{\theta^-_i\theta^-_j}{||\vec{\theta}^-||} \approx 2||\vec{\beta}||n_i n_j.$$

Inserting all of these significantly simplifies our expression for the time delay to the following:

$$\Delta t(\vec{\beta}) \approx \frac{1+z_l}{c}\frac{D_l D_s}{D_{ls}}\Big\{2\theta_E\left[\partial_i\psi_{WL}|_{\vec{\beta}} - \beta_j\partial_i\partial_j\psi_{WL}|_{\vec{\beta}}\right]n_i + 2\theta_E||\vec{\beta}||\partial^2_{\hat{n}}\psi_{WL}|_{\vec{\beta}}$$

$$-2\theta_E(||\vec{\beta}|| + \partial_{\hat{n}}\psi_{WL}|_{\vec{\beta}}) - 2\theta_E\partial_{\hat{n}}\psi_{WL}|_{\vec{\beta}}\Big\}$$

$$= -2\theta_E\frac{1+z_l}{c}\frac{D_l D_s}{D_{ls}}(||\vec{\beta}|| + \partial_{\hat{n}}\psi_{WL}|_{\vec{\beta}}).$$

Insert $\theta_E \equiv \frac{4\pi\sigma_v^2}{c^2}\frac{D_{ls}}{D_s}$ to find

$$\Delta t(\vec{\beta}) = -8\pi(\frac{\sigma_v}{c})^2\frac{\chi_l}{c}(||\vec{\beta}|| + \partial_{\hat{n}}\psi_{WL}|_{\vec{\beta}}).$$

where $\chi_l \equiv (1+z_l)D_l$ is the comoving distance in a flat FLRW universe.

References

[1] J. H. Oort. The force exerted by the stellar system in the direction perpendicular to the galactic plane and some related problems. , 6:249, August 1932.

[2] Vera C. Rubin. Dark matter in spiral galaxies. *Scientific American*, 248(6):96–109, 1983. ISSN 00368733, 19467087. URL http://www.jstor.org/stable/24968923.

[3] F. Zwicky. On the Masses of Nebulae and of Clusters of Nebulae. , 86:217, October 1937. doi: 10.1086/143864.

[4] P. J. E. Peebles and Bharat Ratra. The cosmological constant and dark energy. *Reviews of Modern Physics*, 75(2):559–606, apr 2003. doi: 10.1103/revmodphys.75.559. URL https://doi.org/10.1103%2Frevmodphys.75.559.

[5] N. Aghanim et al. iplanck/i2018 results. *Astronomy &amp Astrophysics*, 641:A6, sep 2020. doi: 10.1051/0004-6361/201833910. URL https://doi.org/10.1051%2F0004-6361%2F201833910.

[6] Bharat Ratra and P. J. E. Peebles. Cosmological consequences of a rolling homogeneous scalar field. *Phys. Rev. D*, 37:3406–3427, Jun 1988. doi: 10.1103/PhysRevD.37.3406. URL https://link.aps.org/doi/10.1103/PhysRevD.37.3406.

[7] C. Armendariz-Picon, V. Mukhanov, and Paul J. Steinhardt. Essentials ofik/i-essence. *Physical Review D*, 63(10), apr 2001. doi: 10.1103/physrevd.63.103510. URL https://doi.org/10.1103%2Fphysrevd.63.103510.

[8] S. Shankaranarayanan and Joseph P. Johnson. Modified theories of gravity: Why, how and what? *General Relativity and Gravitation*, 54(5), may 2022. doi: 10.1007/s10714-022-02927-2. URL https://doi.org/10.1007%2Fs10714-022-02927-2.

[9] S. Nojiri, S.D. Odintsov, and V.K. Oikonomou. Modified gravity theories on a nutshell: Inflation, bounce and late-time evolution. *Physics Reports*, 692:1–104, jun 2017. doi: 10.1016/j.physrep.2017.06.001. URL https://doi.org/10.1016%2Fj.physrep.2017.06.001.

[10] K.C. Wong et al. H0licow – XIII. a 2.4 per cent measurement of h0 from lensed quasars: 5.3 tension between early- and late-universe probes. *Monthly Notices of the Royal Astronomical Society*, 498(1):1420–1439, sep 2019. doi: 10.1093/mnras/stz3094. URL https://doi.org/10.1093%2Fmnras%2Fstz3094.

[11] Florian Niedermann and Martin S. Sloth. Resolving the hubble tension with new early dark energy. *Physical Review D*, 102(6), sep 2020. doi: 10.1103/physrevd.102.063527. URL https://doi.org/10.1103%2Fphysrevd.102.063527.

[12] Laura Herold and Elisa G. M. Ferreira. Resolving the hubble tension with early dark energy, 2022. URL https://arxiv.org/abs/2210.16296.

[13] Planck Collaboration et al. Planck 2013 results. XV. CMB power spectra and likelihood. , 571:A15, November 2014. doi: 10.1051/0004-6361/201321573.

[14] E. Keihänen, H. Kurki-Suonio, V. Lindholm, A. Viitanen, A.-S. Suur-Uski, V. Allevato, E. Branchini, F. Marulli, P. Norberg, D. Tavagnacco, S. de la Torre, J. Valiviita, M. Viel, J. Bel, M. Frailis, and A. G. Sá nchez. Estimating the galaxy two-point correlation function using a split random catalog. *Astronomy &amp Astrophysics*, 631:A73, oct 2019. doi: 10.1051/0004-6361/201935828. URL https://doi.org/10.1051%2F0004-6361%2F201935828.

[15] Ulf Leonhardt. Wave correlations and quantum noise in cosmology. *Journal of Physics A: Mathematical and Theoretical*, 56(2):024001, jan 2023. doi: 10.1088/1751-8121/acb027. URL https://doi.org/10.1088%2F1751-8121%2Facb027.

[16] Draž en Glavan, Tomislav Prokopec, and Tomo Takahashi. Late-time quantum backreaction of a very light nonminimally coupled scalar. *Physical Review D*, 94(8), oct 2016. doi: 10.1103/physrevd.94.084053. URL https://doi.org/10.1103%2Fphysrevd.94.084053.

[17] Dražen Glavan, Tomislav Prokopec, and Alexei A. Starobinsky. Stochastic dark energy from inflationary quantum fluctuations. *The European Physical Journal C*, 78(5), may 2018. doi: 10.1140/epjc/s10052-018-5862-5. URL https://doi.org/10.1140%2Fepjc%2Fs10052-018-5862-5.

[18] Marek Demianski and Ester Piedipalumbo. Observational tests of the Glavan, Prokopec and Starobinsky model of dark energy. *The European Physical Journal C*, 79(7), jul 2019. doi: 10.1140/epjc/s10052-019-7045-4. URL https://doi.org/10.1140%2Fepjc%2Fs10052-019-7045-4.

[19] Enis Belgacem and Tomislav Prokopec. Spatial correlations of dark energy from quantum fluctuations during inflation. *Physical Review D*, 106(12), dec 2022. doi: 10.1103/physrevd.106.123514. URL https://doi.org/10.1103%2Fphysrevd.106.123514.

[20] Željko Ivezić et al. LSST: From Science Drivers to Reference Design and Anticipated Data Products. , 873(2):111, March 2019. doi: 10.3847/1538-4357/ab042c.

[21] R. Arnowitt, S. Deser, and C. W. Misner. Dynamical Structure and Definition of Energy in General Relativity. *Physical Review*, 116(5):1322–1330, December 1959. doi: 10.1103/PhysRev.116.1322.

[22] Scott Dodelson. *Modern Cosmology*. Academic Press, Elsevier Science, 2003.

[23] S. Birrer, M. Millon, D. Sluse, A. J. Shajib, F. Courbin, L. V. E. Koopmans, S. H. Suyu, and T. Treu. Time-delay cosmography: Measuring the hubble constant and other cosmological parameters with strong gravitational lensing, 2023.

[24] Rennan Barkana. Fast calculation of a family of elliptical gravitational lens models. *The Astrophysical Journal*, 502(2):531–537, aug 1998. doi: 10.1086/305950. URL https://doi.org/10.1086%2F305950.

[25] G. Hinshaw, D. N. Spergel, L. Verde, R. S. Hill, S. S. Meyer, C. Barnes, C. L. Bennett, M. Halpern, N. Jarosik, A. Kogut, E. Komatsu, M. Limon, L. Page, G. S. Tucker, J. L. Weiland, E. Wollack, and E. L. Wright. First-year wilkinson microwave anisotropy probe (wmap)* observations: The angular power spectrum. *The Astrophysical Journal Supplement Series*, 148(1):135, sep 2003. doi: 10.1086/377225. URL https://dx.doi.org/10.1086/377225.

[26] Yury Petrov. Harmony: Eeg/meg linear inverse source reconstruction in the anatomical basis of spherical harmonics. *PloS one*, 7:e44439, 10 2012. doi: 10.1371/journal.pone.0044439.

[27] Masamune Oguri and Philip J. Marshall. Gravitationally lensed quasars and supernovae in future wide-field optical imaging surveys. *Monthly Notices of the Royal Astronomical Society*, pages no–no, apr 2010. doi: 10.1111/j.1365-2966.2010.16639.x. URL https://doi.org/10.1111%2Fj.1365-2966.2010.16639.x.

[28] A. A. Starobinsky. Stochastic de sitter (inflationary) stage in the early universe. In H. J. de Vega and N. Sánchez, editors, *Field Theory, Quantum Gravity and Strings*, pages 107–126, Berlin, Heidelberg, 1986. Springer Berlin Heidelberg. ISBN 978-3-540-39789-2.

[29] Daniel Baumann. Tasi lectures on primordial cosmology, 2018.

[30] Contents. In Scott Dodelson and Fabian Schmidt, editors, *Modern Cosmology (Second Edition)*, pages v–xii. Academic Press, second edition edition, 2021. ISBN 978-0-12-815948-4. doi: https://doi.org/10.1016/B978-0-12-815948-4.00004-8. URL https://www.sciencedirect.com/science/article/pii/B9780128159484000048.

[31] Nora Elisa Chisari and Andrew Pontzen. Unequal time correlators and the zel'dovich approximation. *Physical Review D*, 100(2), jul 2019. doi: 10.1103/physrevd.100.023543. URL https://doi.org/10.1103%2Fphysrevd.100.023543.